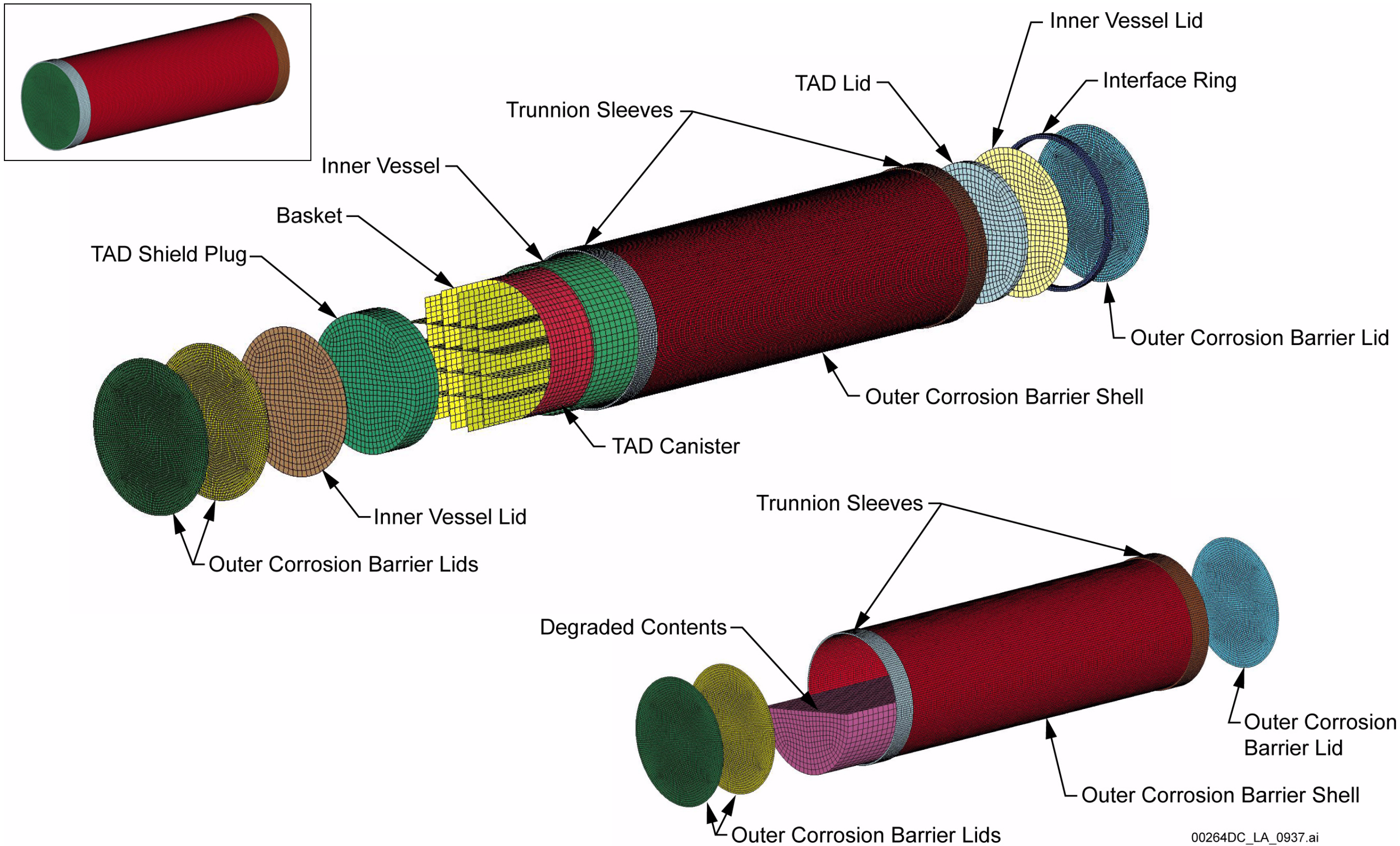


Figure 2.3.4-54. Detailed Representation of the TAD-Bearing Waste Package with Intact and Degraded Internals Used for Waste Package Damage Lookup Table Analyses

NOTE: These models accurately reflect the design of the Naval-Long waste package and an approximate representation of a TAD canister and fuel basket at the time the computational model was developed. *Mechanical Assessment of Degraded Waste Packages and Drip Shields Subject to Vibratory Ground Motion* (SNL 2007b, Section 6.3.2.2.1) is a stylized rendition that does not represent any of the TAD designs currently in “full and open competition” procurement by DOE. In addition, minor design changes have subsequently occurred for the Naval-Long waste package, such as removed of the inner lid, which are not anticipated to have a significant impact on damaged areas.

Source: SNL 2007b, Figures 6-12 and 6-13.

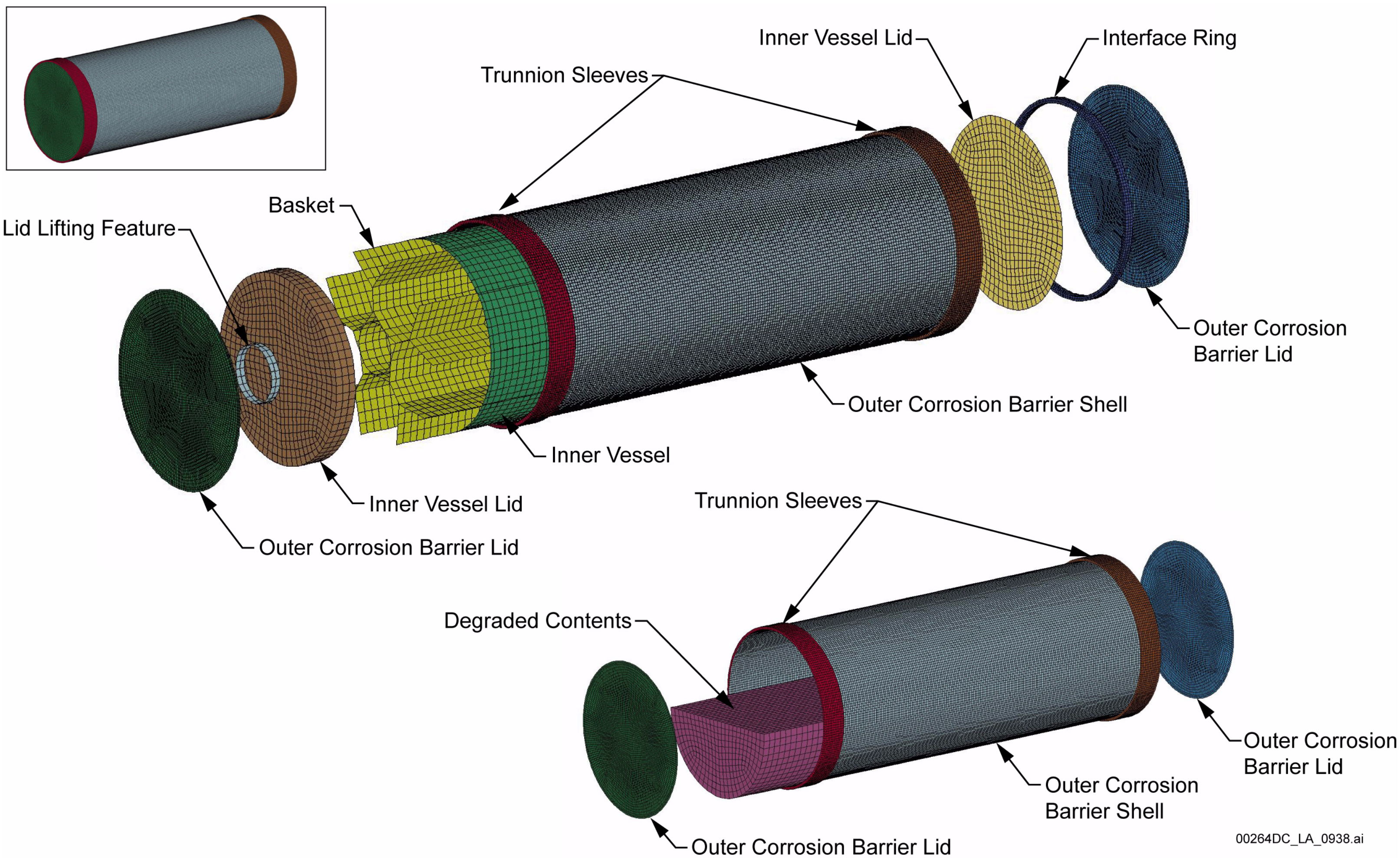


Figure 2.3.4-55. Detailed Representation of the Codisposal Waste Package with Intact and Degraded Internals Used for Waste Package Damage Lookup Table Analyses

NOTE: These models accurately reflect the codisposal waste package design at the time of the development of these calculations.

Source: SNL 2007b, Figures 6-14 and 6-15.

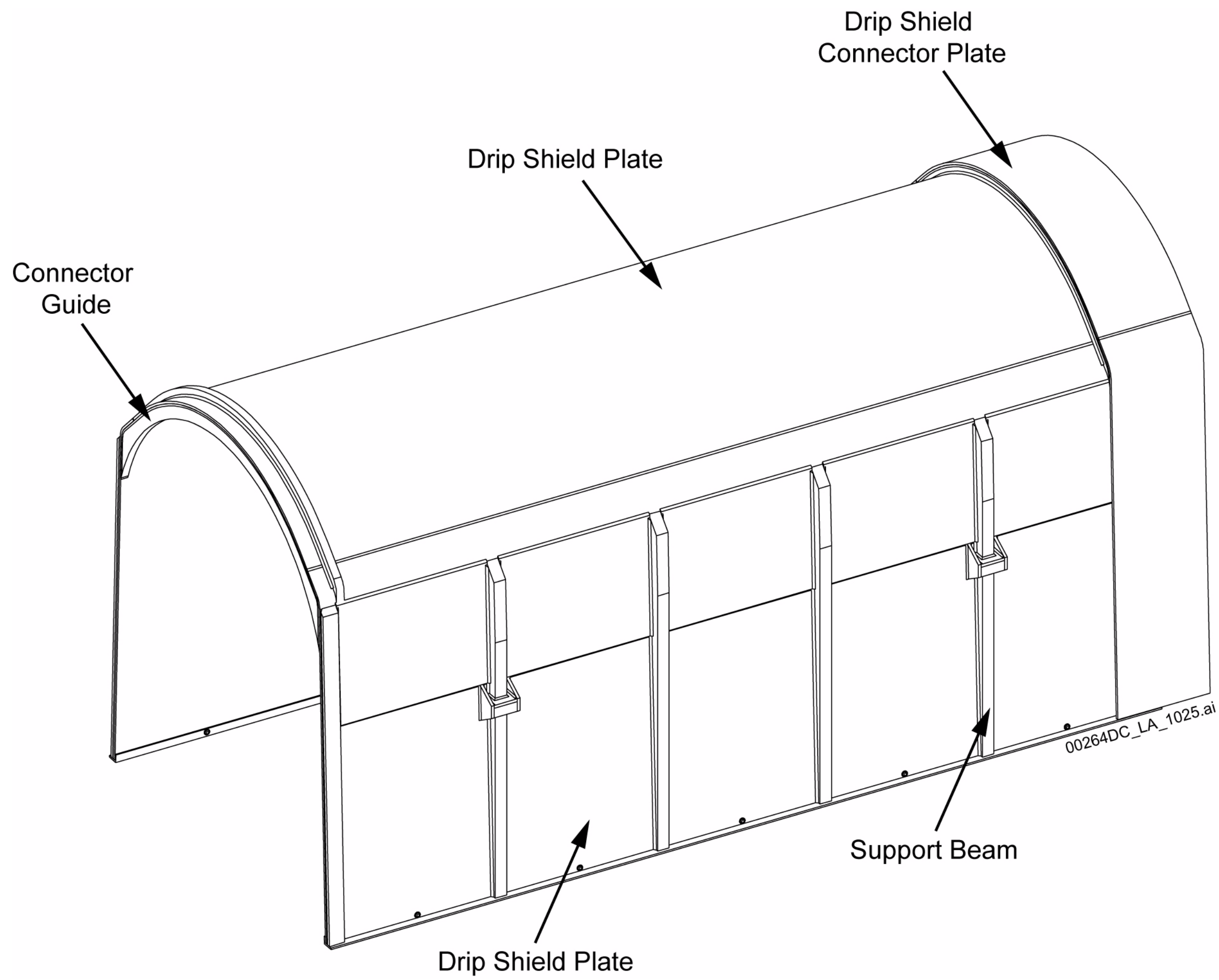


Figure 2.3.4-56. Simplified Isometric of the Drip Shield

NOTE: For design details, see Figures 1.3.4-14 and 1.3.4-15.

Source: SNL 2007c, Figure 6-3.

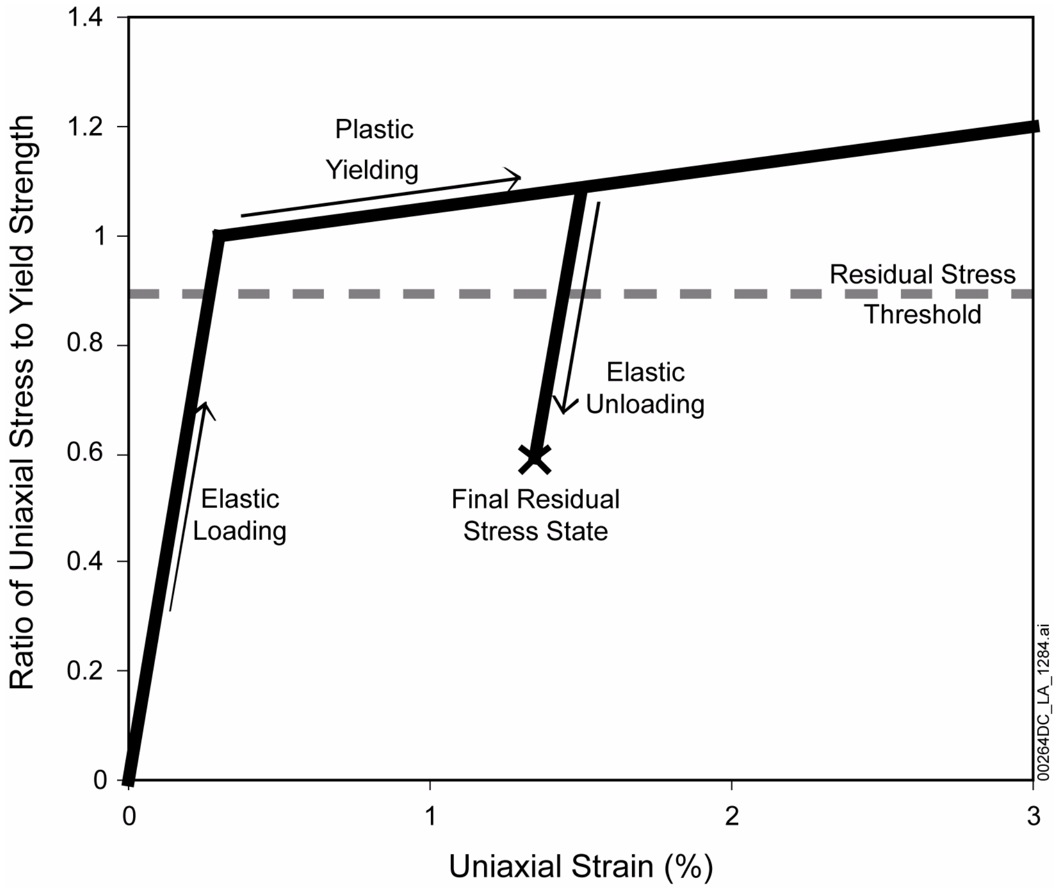


Figure 2.3.4-57. Permanent Deformation from Plastic Yielding Generates Residual Stress

Source: SNL 2007c, Figure 6-5.

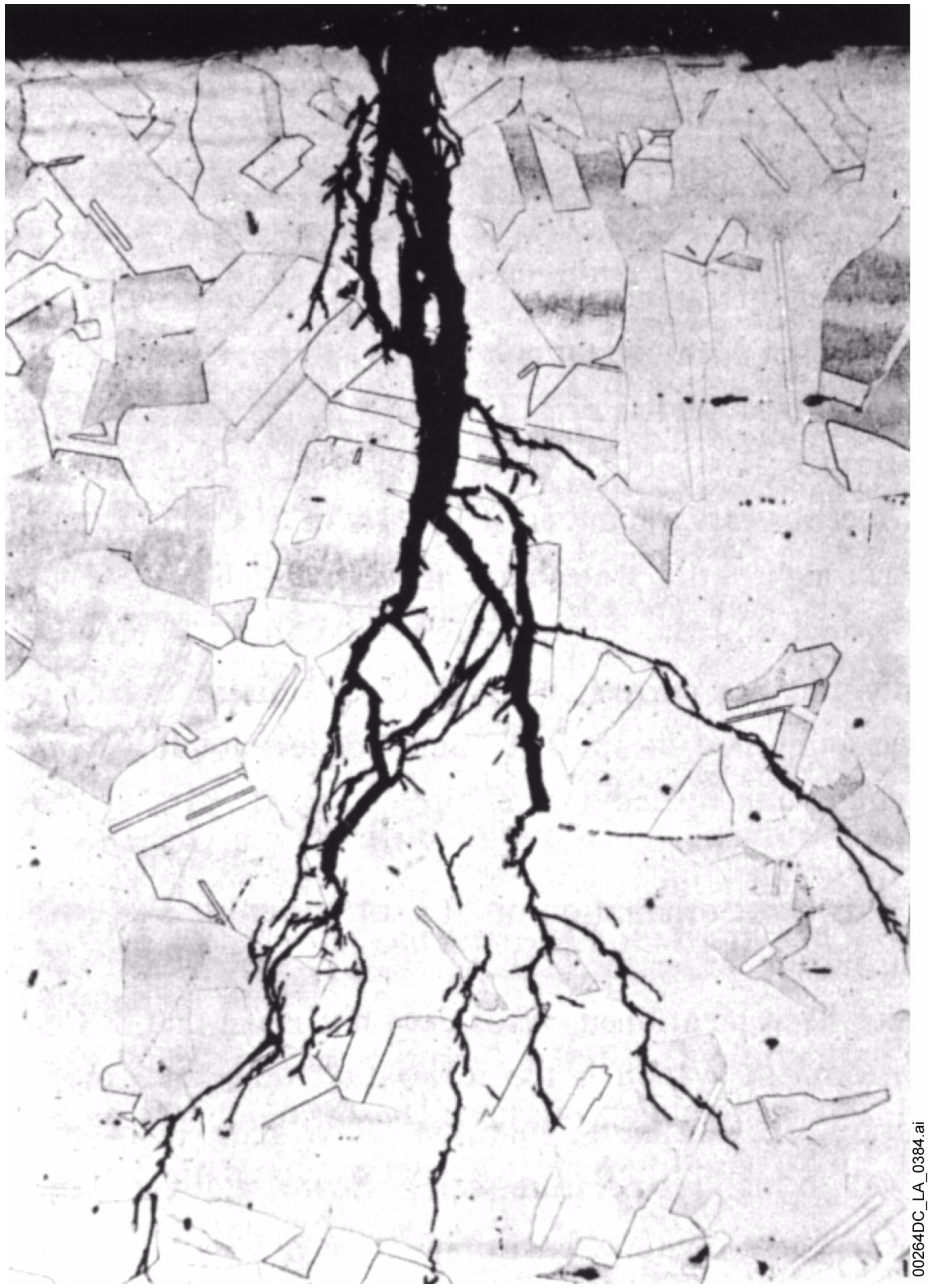


Figure 2.3.4-58. Typical Example of Transgranular Stress Corrosion Crack in Stainless Steel

NOTE: Magnification is 216×.

Source: SNL 2007a, Figure 6-61.

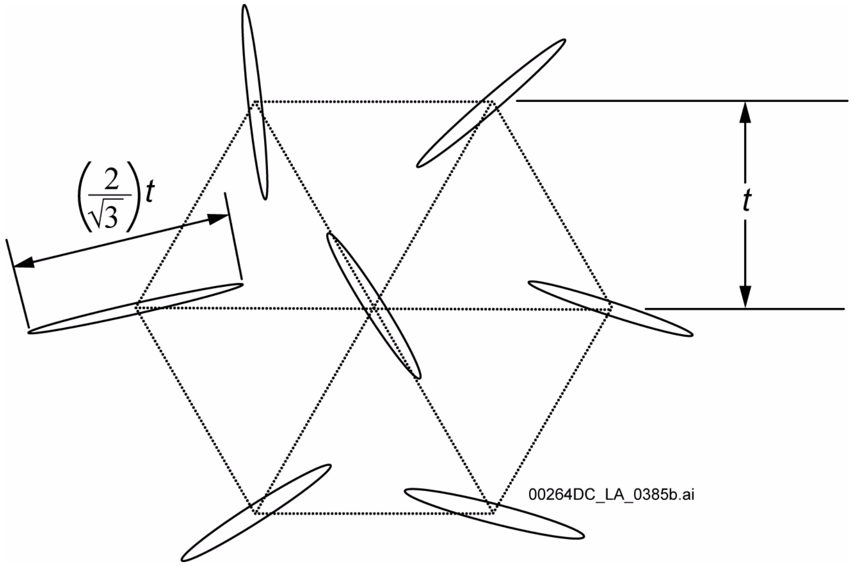


Figure 2.3.4-59. Parallel Rows of Randomly Oriented Flaws, with Row Spacing Equal to Wall Thickness

NOTE: Drawing not to scale.

Source: SNL 2007a, Figure 6-63.

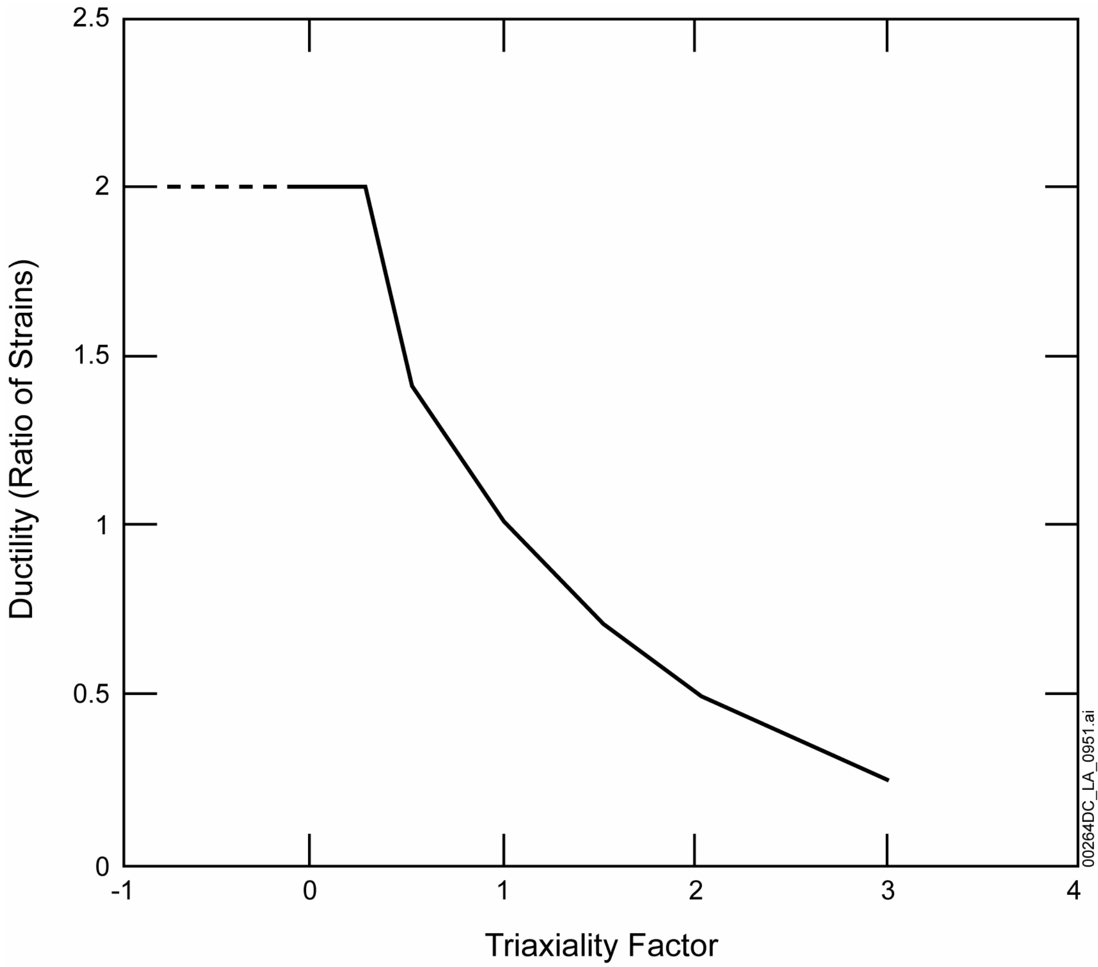


Figure 2.3.4-60. Ductility Ratio vs. Triaxiality Factor

Source: NNSA 2005, Appendix M.

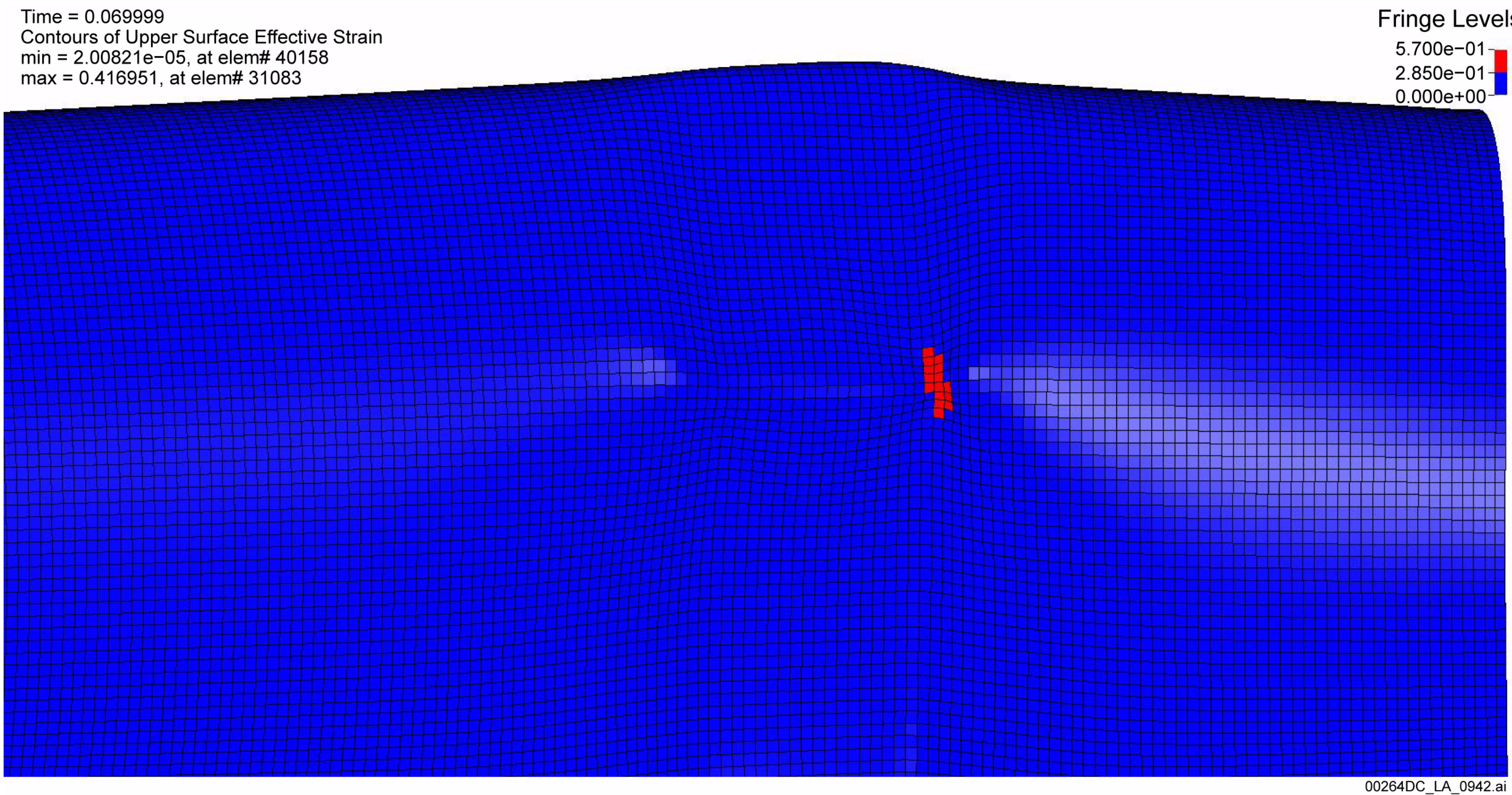


Figure 2.3.4-61. Example of a Fringe Plot Showing the Area of a Dented Outer Corrosion Barrier Surface Shell with Elements with Effective Strains Exceeding 0.285

NOTE: TAD-bearing waste package, 23 mm outer corrosion barrier with degraded internals, 10 m/s impact. This is the highest impact velocity examined.

Source: SNL 2007b, Figure 6-27.

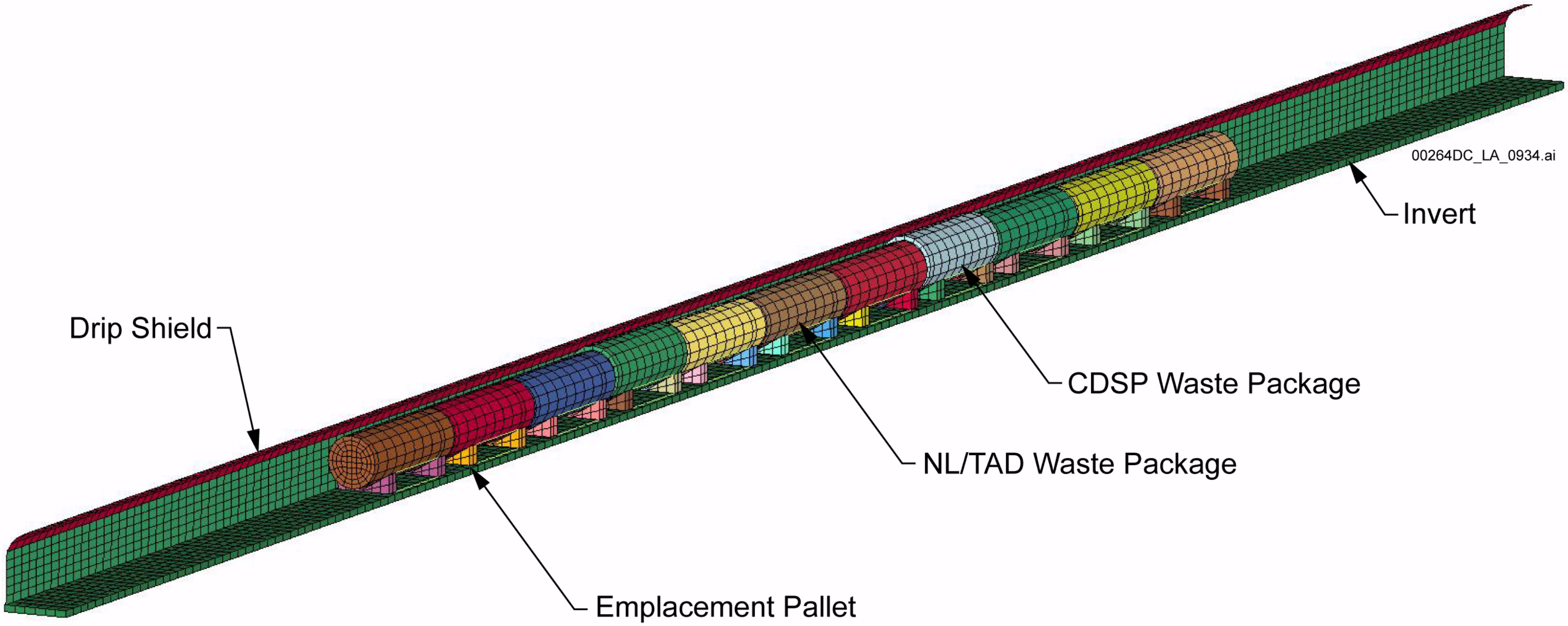


Figure 2.3.4-62. Eleven Waste Package Configuration for Focus on Central Three TAD-Bearing Waste Packages (One Side of the Drip Shield is Removed for Clarity)

NOTE: The configuration consists of nine TAD-bearing packages and two codisposal waste packages. Impacts to the center three packages are considered representative of a typical repository TAD-bearing waste package.

Source: SNL 2007b, Figure 6-3.

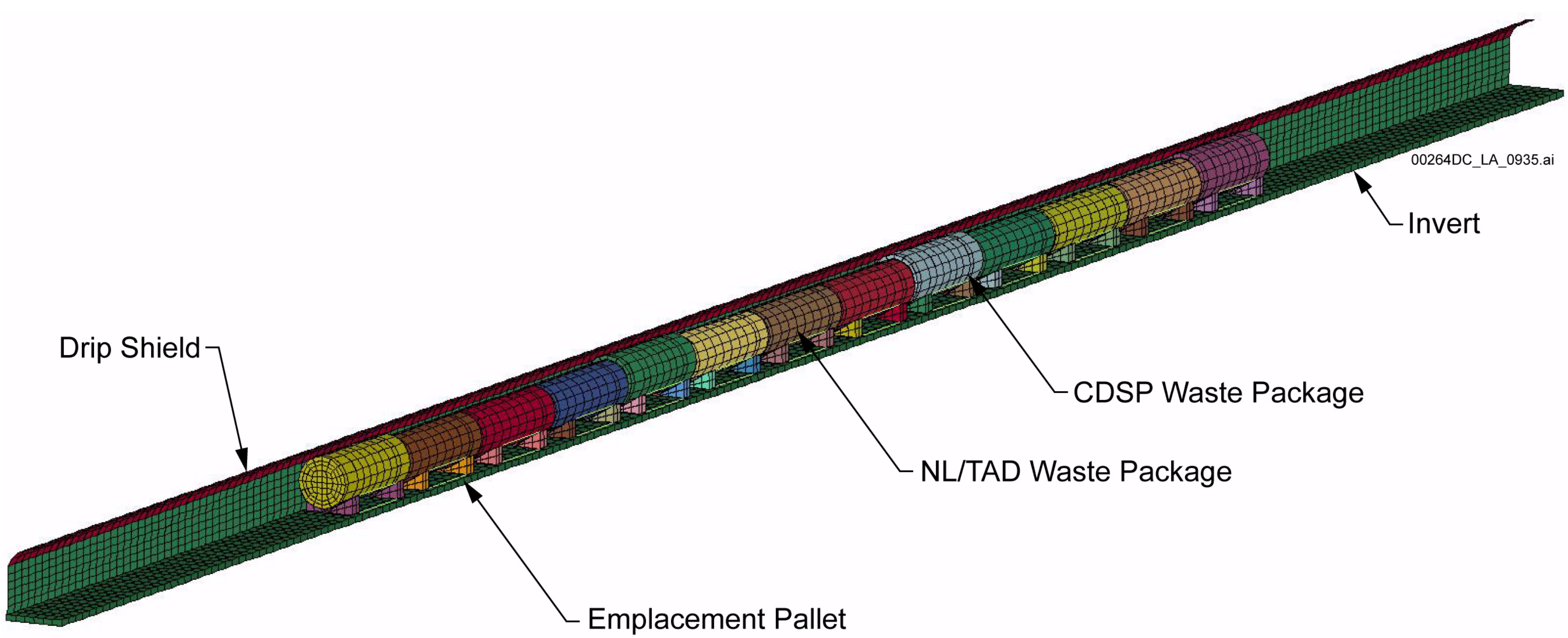


Figure 2.3.4-63. Thirteen Waste Package Configuration for Focus on Central Two Codisposal Waste Packages. (One Side of the Drip Shield is Removed for Clarity)

NOTE: The configuration consists of nine TAD-bearing packages and four codisposal waste packages. Impacts to the two central codisposal waste packages are considered representative of a typical repository codisposal waste package.

Source: SNL 2007b, Figure 6-4.

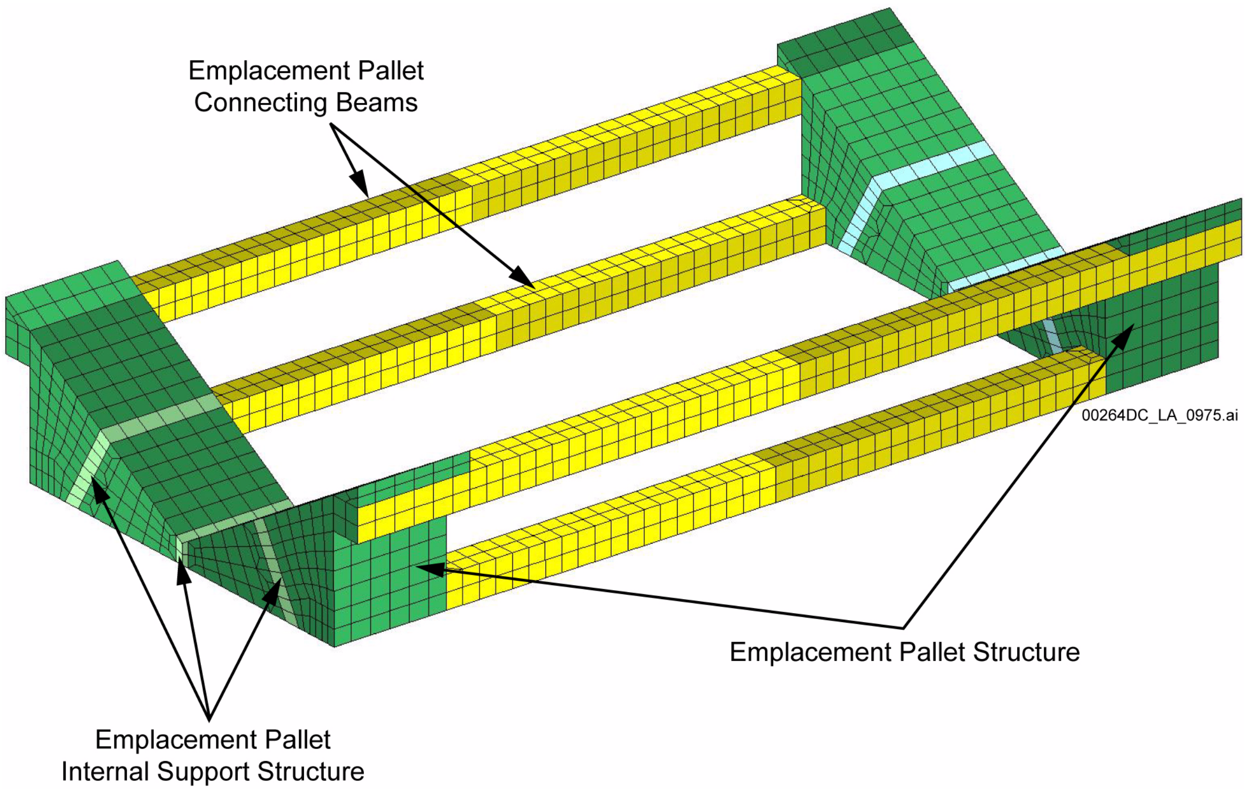


Figure 2.3.4-64. Detailed Representation of the Emplacement Pallet Used for Waste Package Damage Lookup Table Analyses. The Connecting Beams are Removed for Analyses with Degraded Internals.

Source: SNL 2007b, Figure 6-16.


Figure 2.3.4-65. Example of Impact Location Configurations for TAD-Bearing Waste Package-to-TAD-Bearing Waste Package Damage Lookup Table Analyses. All Analyses Were Performed with an Impact Angle of 1.5 Degrees.

Source: SNL 2007b, Figure 6-17.

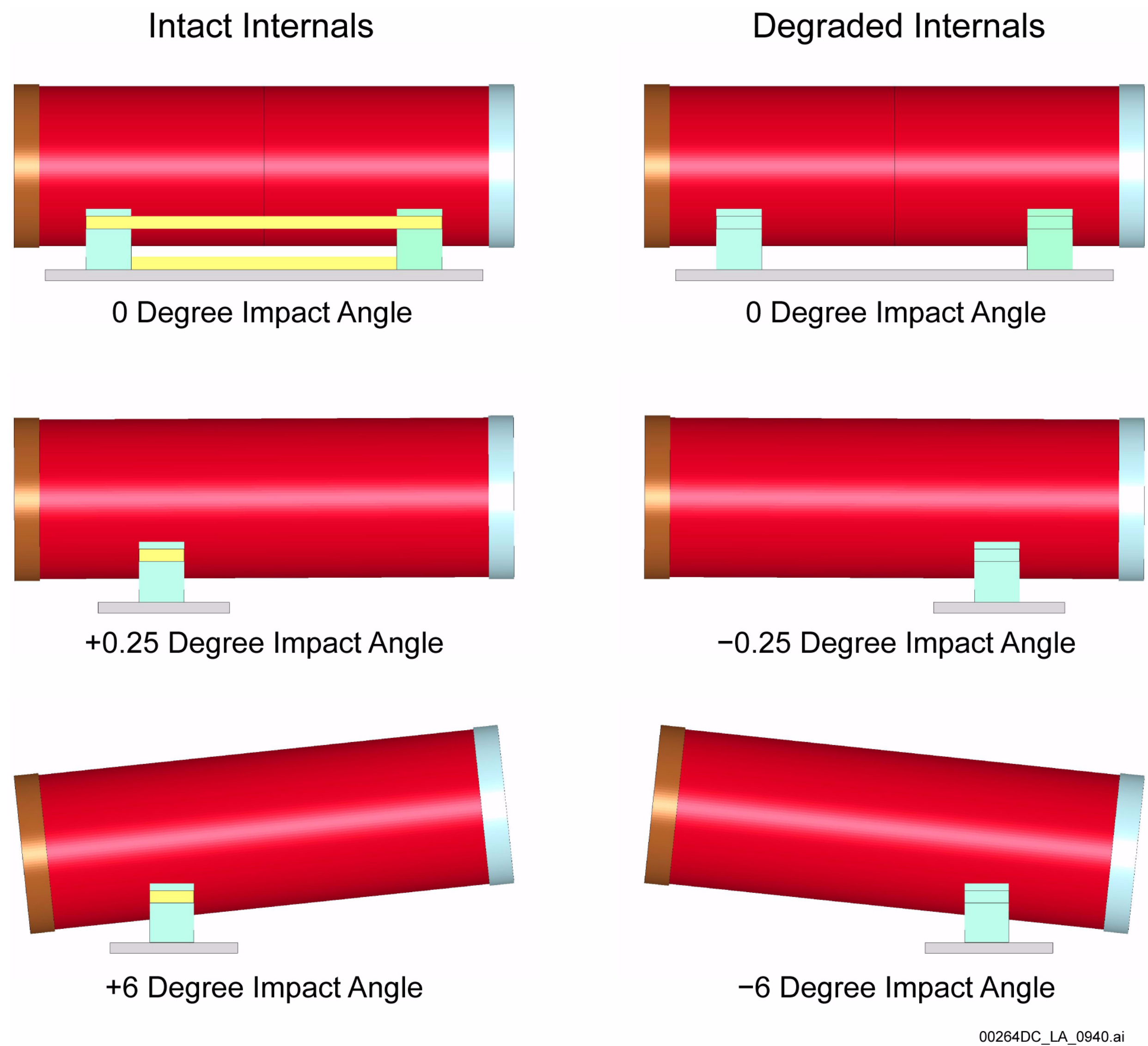


Figure 2.3.4-66. Representative Impact Angle Configurations for Waste Package-to-Pallet Damage Lookup Table Analyses for the TAD-Bearing (shown) and Codisposal Waste Package

Source: SNL 2007b, Figure 6-20.

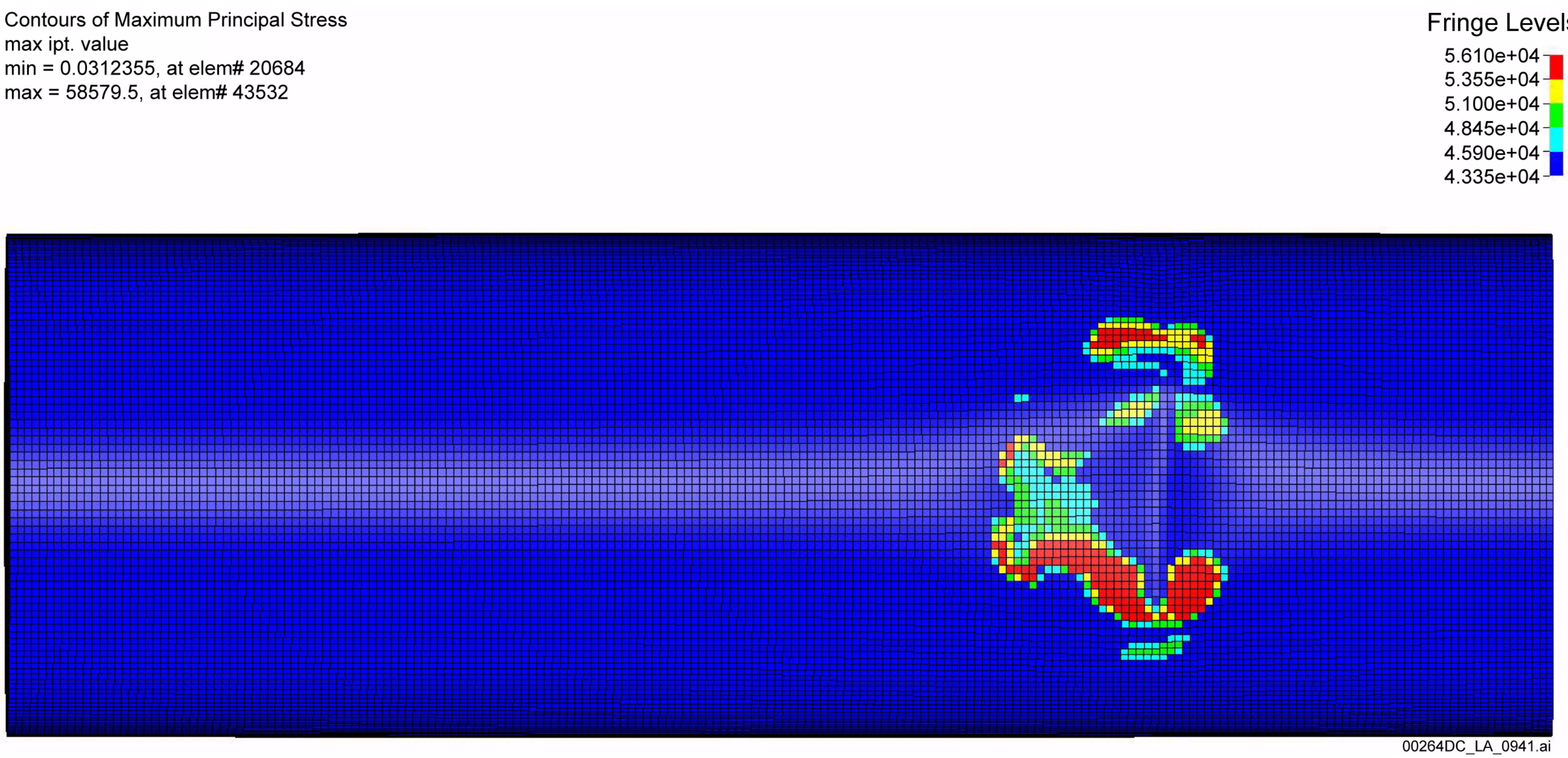


Figure 2.3.4-67. Example of Damaged Area Resulting from Waste Package-to-Pallet Impacts, Contoured on the Lower Hemicylinder of a Waste Package Outer Corrosion Barrier

NOTE: The dark blue is below 90% of yield strength; the light blue, green, yellow and red combined are above 90% of yield strength; the yellow and red combined are above 100% of yield strength; and the red is above 105% of yield strength. TAD-bearing waste package, 23 mm outer corrosion barrier, degraded internals, 3 m/s impact velocity.

Source: SNL 2007b, Figure 6-24.

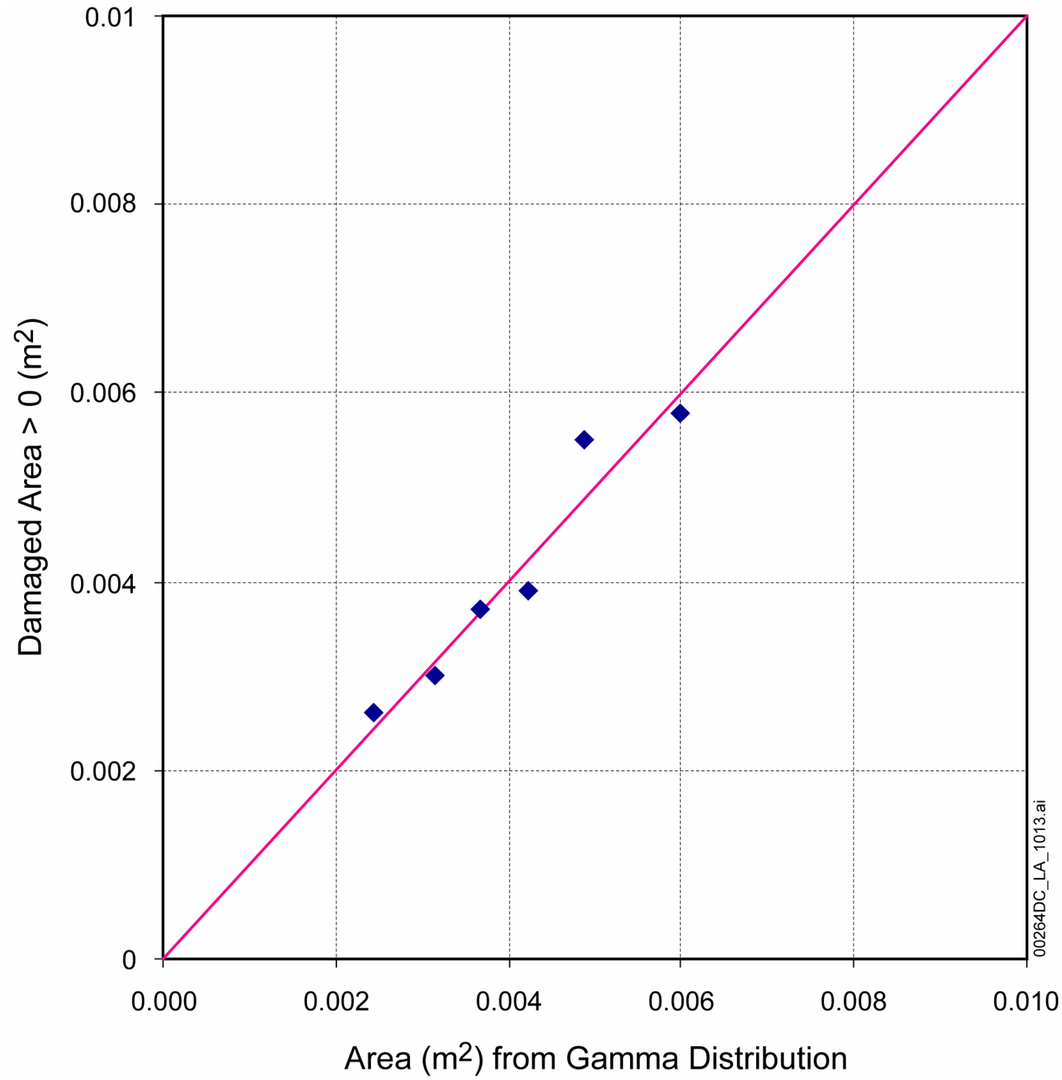


Figure 2.3.4-68. Q-Q Plot for Conditional Nonzero Damaged Areas Versus a Gamma Distribution for the TAD-Bearing Waste Package with 23-mm-Thick Outer Corrosion Barrier and Intact Internals

NOTE: 4.07 m/s PGV level at 90% RST. Damaged area > 0 is the conditional nonzero damaged area.

Source: SNL 2007c, Figure 6-9.

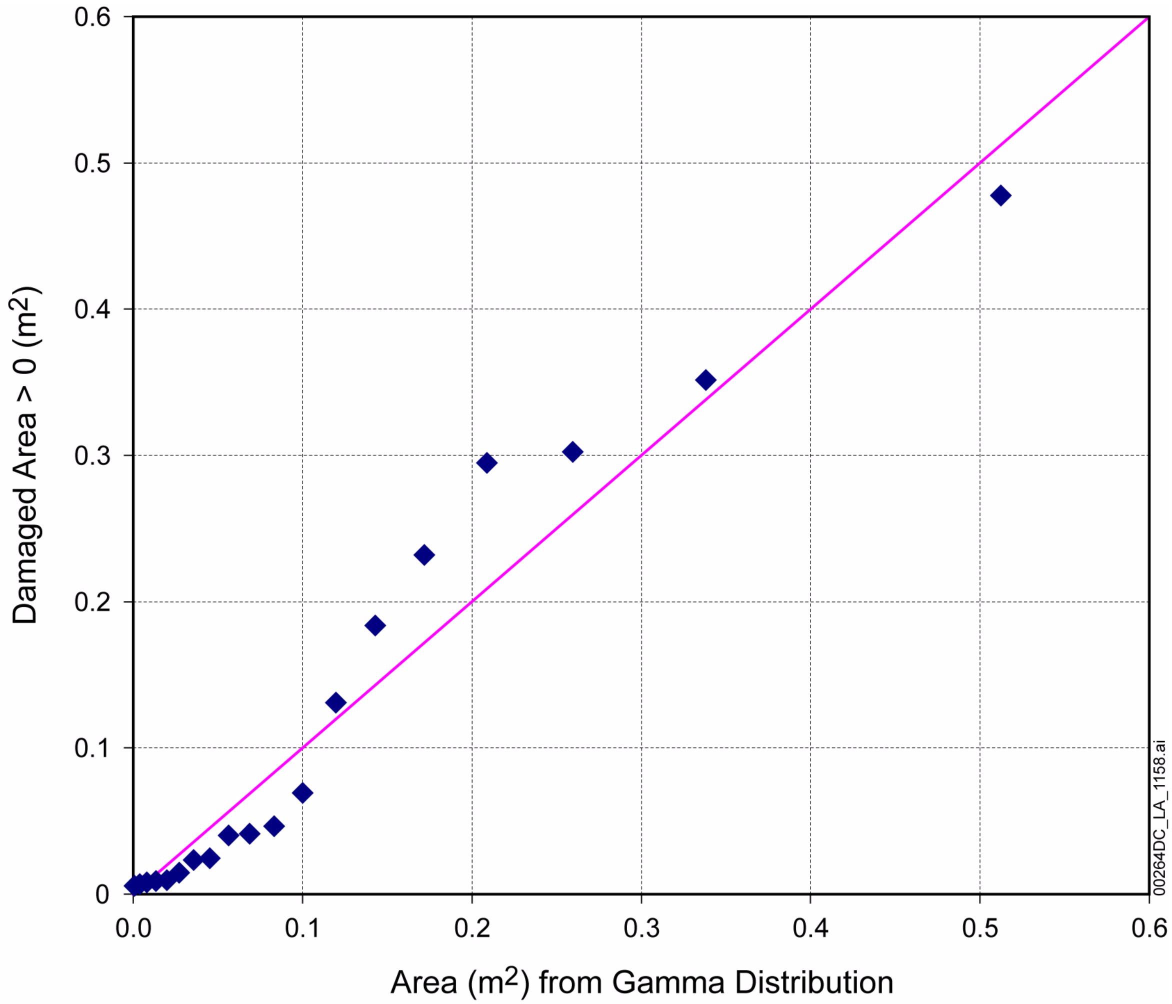


Figure 2.3.4-69. Q-Q Plot for Conditional Damaged Areas Versus a Gamma Distribution for the Codisposal Waste Package with 23-mm-Thick Outer Corrosion Barrier and Intact Internals

NOTE: Damaged area > 0 is the conditional nonzero damaged area. 1.05 PGV level at 90% RST. Damaged Area > 0 is the conditional nonzero damaged area.

Source: SNL 2007c, Figure 6-29.

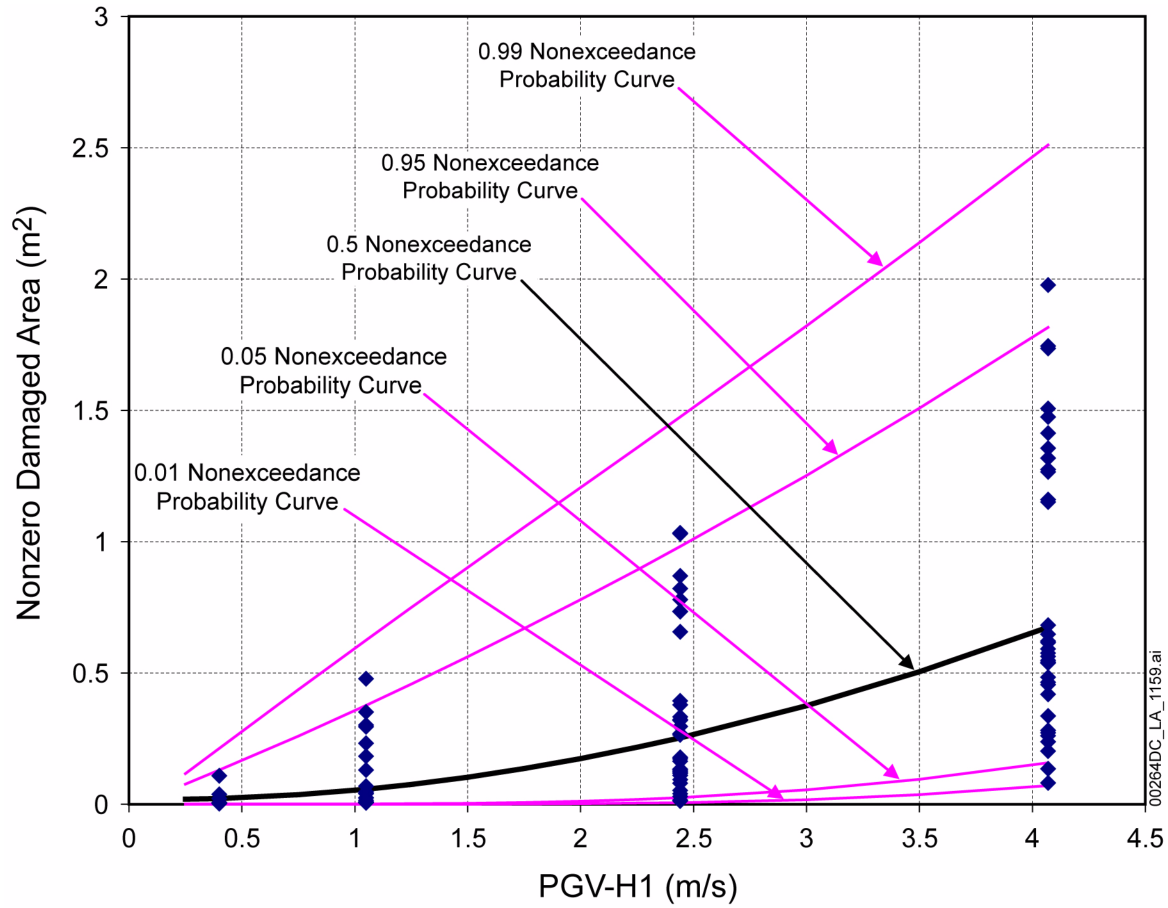


Figure 2.3.4-70. Comparison of Percentiles on the Gamma Distributions to Conditional Damaged Areas for the Codisposal Waste Package with 23-mm-Thick Outer Corrosion Barrier and Intact Internals

Source: SNL 2007c, Figure 6-33.

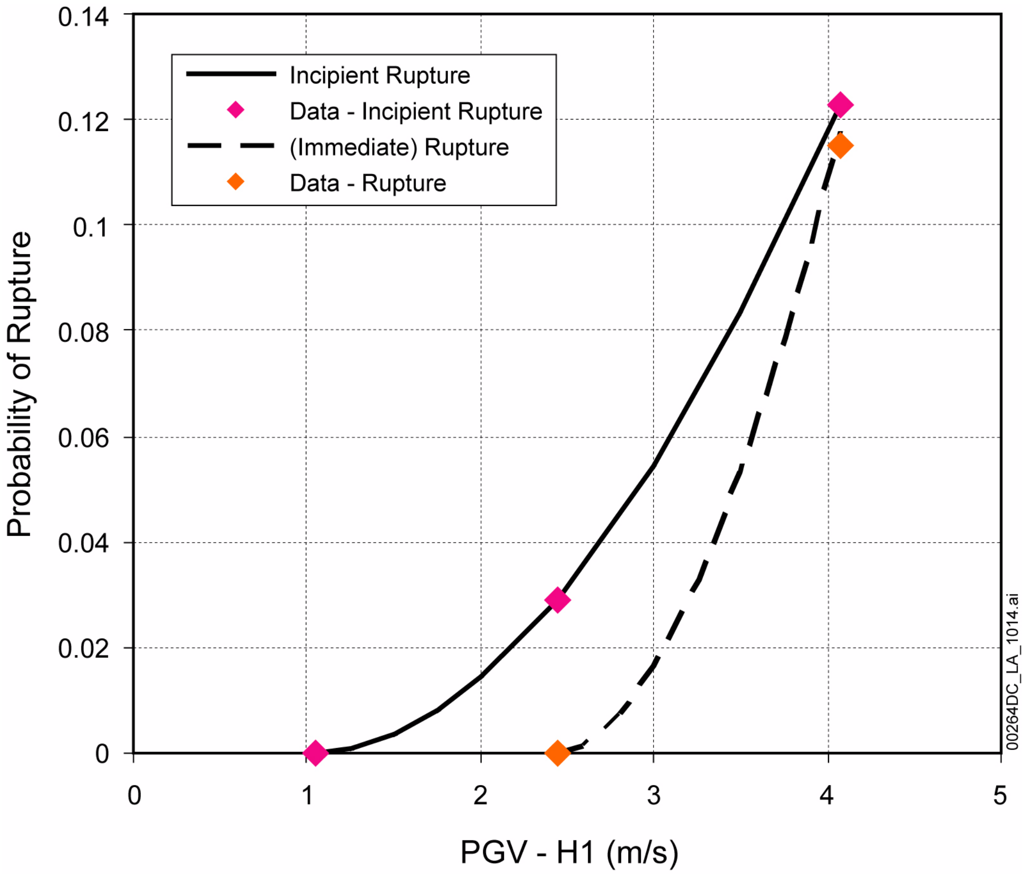


Figure 2.3.4-71. Comparison of Power Law Dependence with Probability Data for Incipient Rupture and for Rupture

NOTE: Kinematic response of codisposal waste package with degraded internals.

Source: SNL 2007c, Figure 6-38.

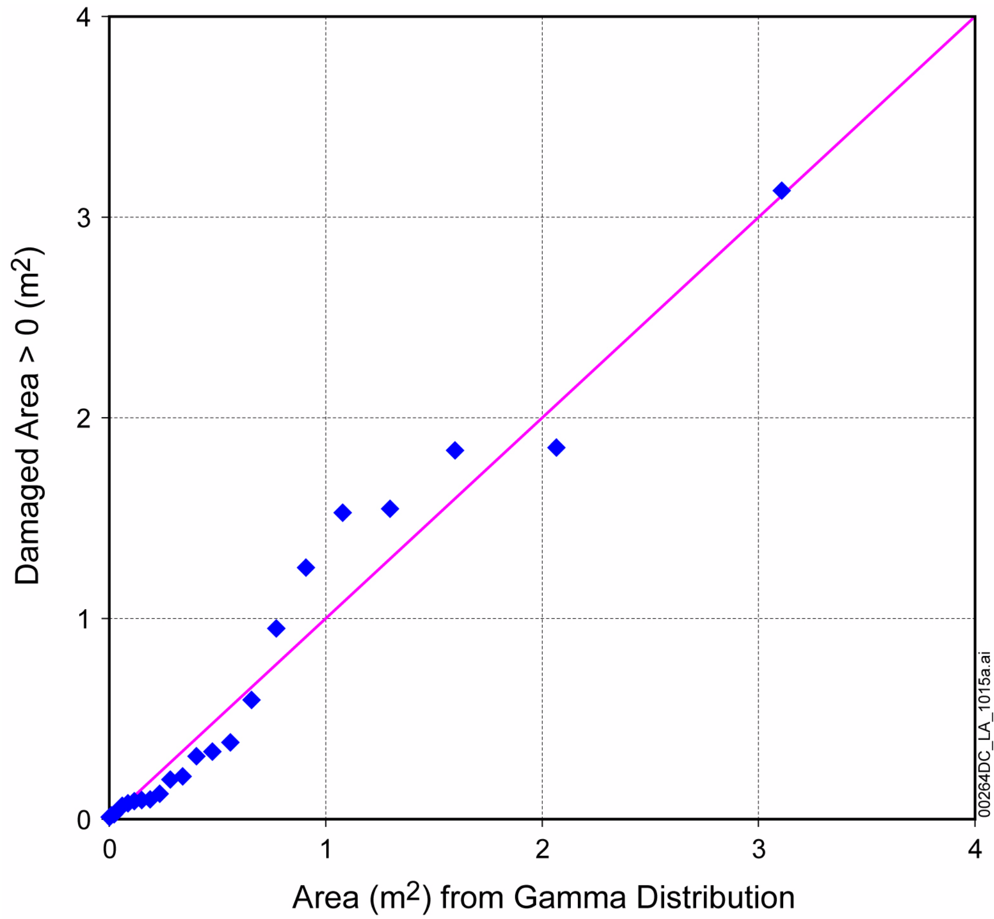


Figure 2.3.4-72. Q-Q Plots for Conditional Damaged Areas Versus a Gamma Distribution for the Codisposal Waste Package with 17-mm-Thick Outer Corrosion Barrier and Degraded Internals

NOTE: Damaged area > 0 is the conditional nonzero damaged area. 1.05 m/s PGV level at 90% RST. Damaged Area > 0 is the conditional nonzero damaged area

Source: SNL 2007c, Figure 6-42.

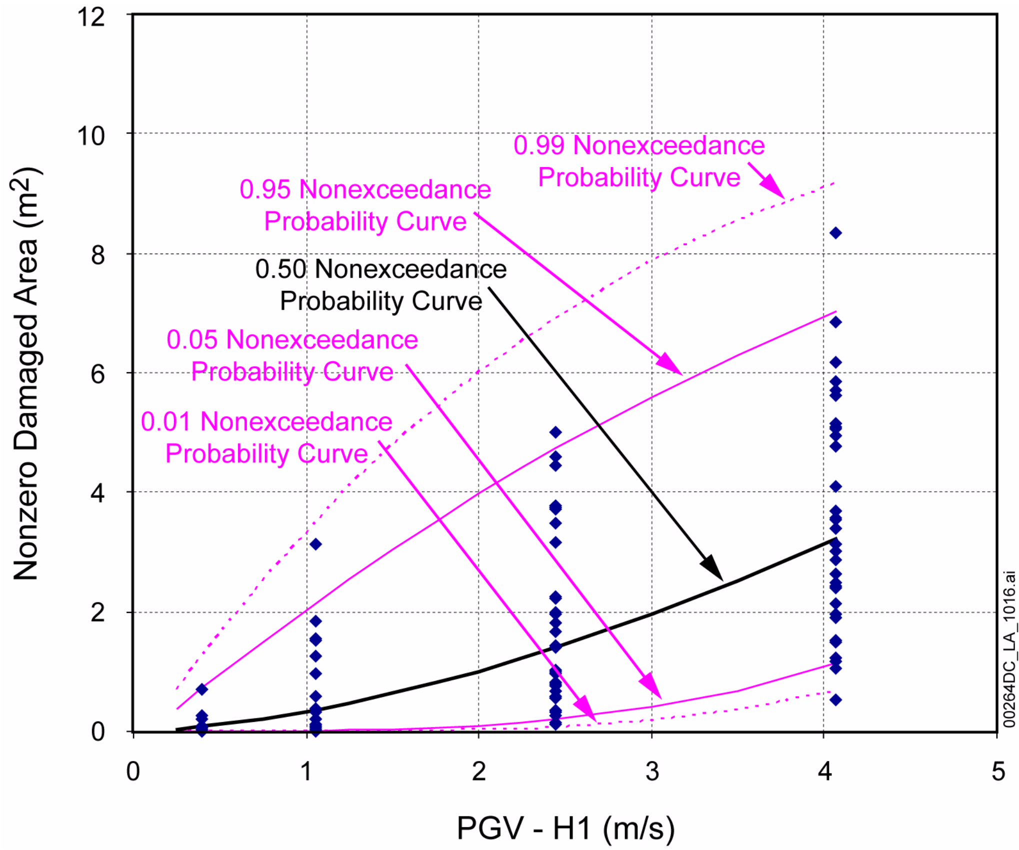


Figure 2.3.4-73. Comparison of Percentiles on the Gamma Distributions to Conditional Damaged Areas for the Codisposal Waste Package with 17-mm-Thick Outer Corrosion Barrier and Degraded Internals

NOTE: 90% RST.

Source: SNL 2007c, Figure 6-46.

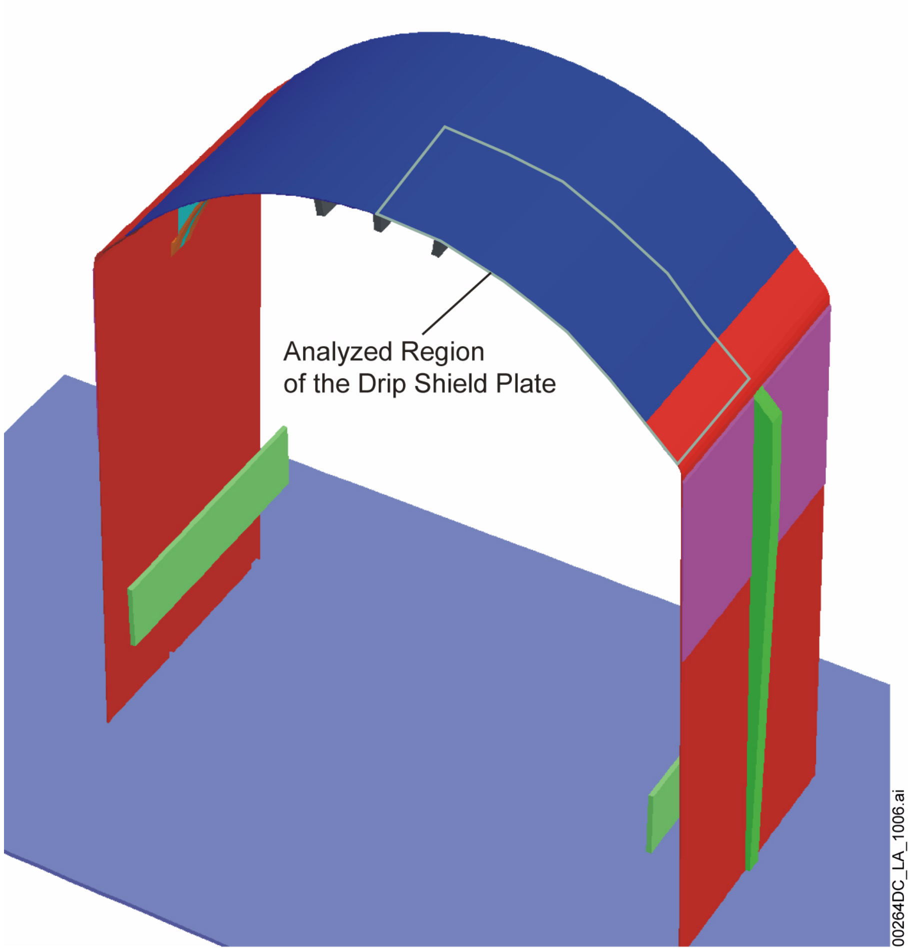


Figure 2.3.4-74. Drip Shield Geometry Showing the Outline of the Region of the Crown Plate for Which Structural Response to Rubble Loading Was Determined

NOTE: Horizontal green plates inside the drip shield are boundary conditions representing the pallet.

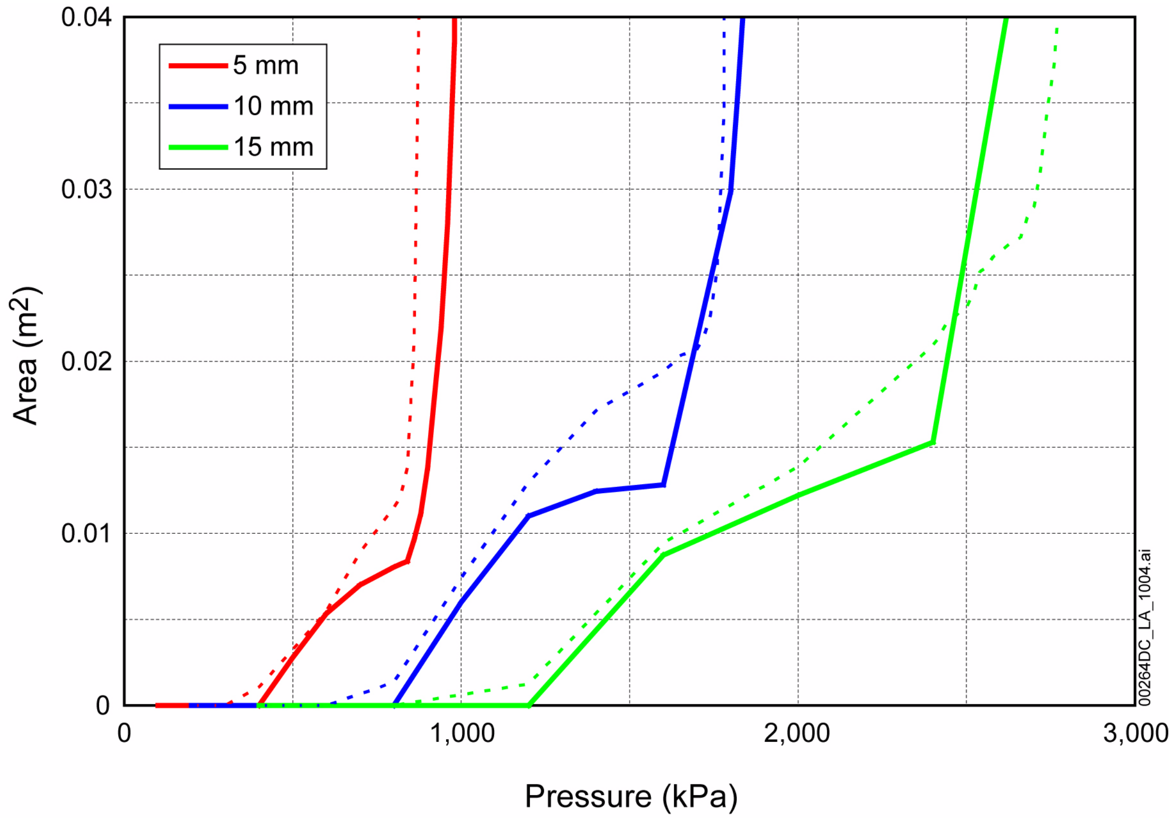


Figure 2.3.4-75. Damage Areas in the Drip Shield Plate as a Function of Uniform Load for Different Plate Thicknesses and Boundary Conditions

NOTE: The solid line is for the Case 1 boundary condition; the thin, dashed line is for the Case 2 boundary condition. The reported results are for the analyzed segment of the drip shield crown plate-i.e., the segment between the bulkhead, the plane of symmetry between the bulkheads, the middle stiffener and the drip shield shoulder. To obtain the damage for the entire drip shield, the results need to be multiplied by 20.

Source: SNL 2007b, Figure 6-43.

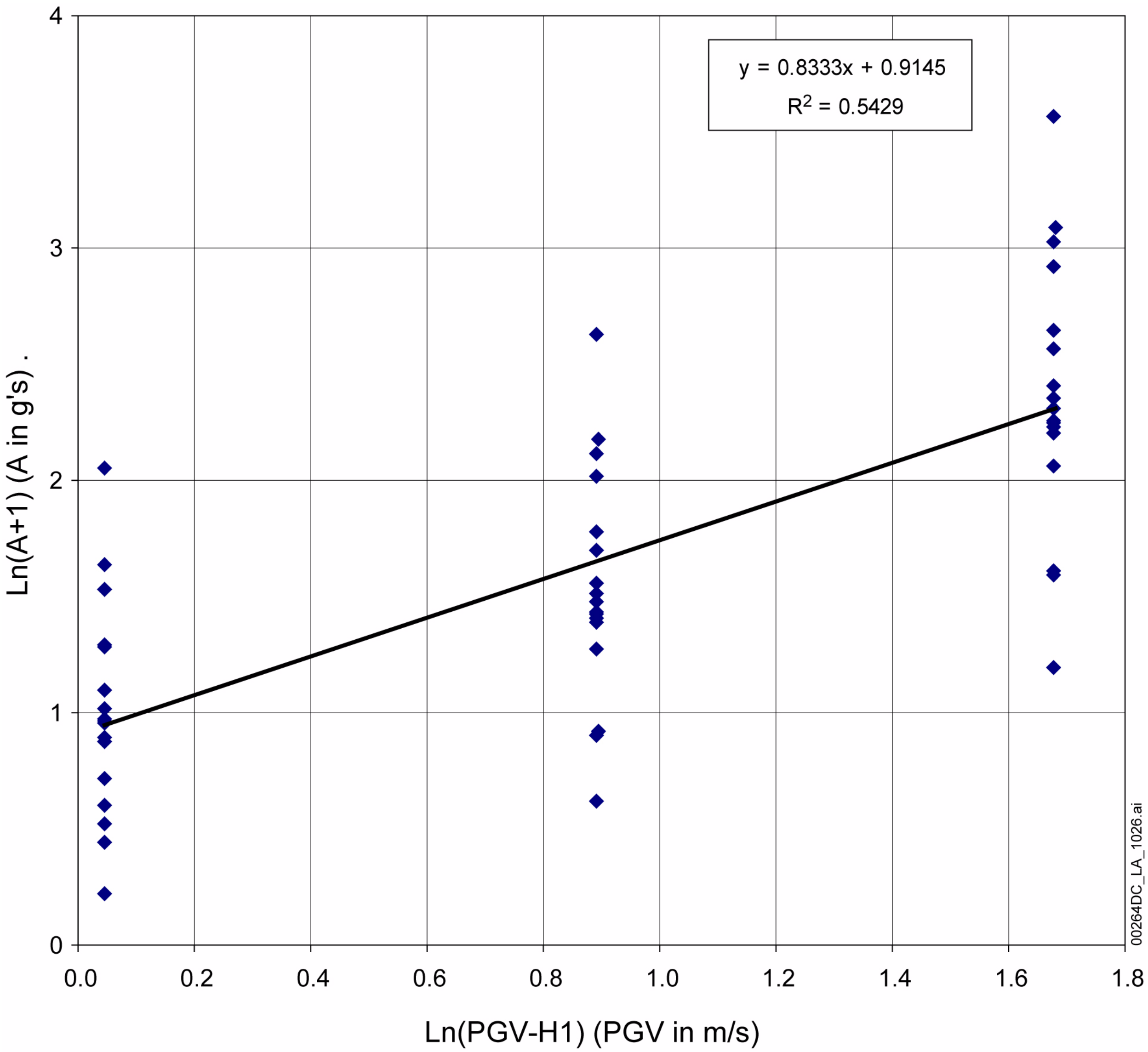


Figure 2.3.4-76. Linear Fit to Ln(A+1) Versus Ln (PGV)

Source: SNL 2007c, Figure 6-92.

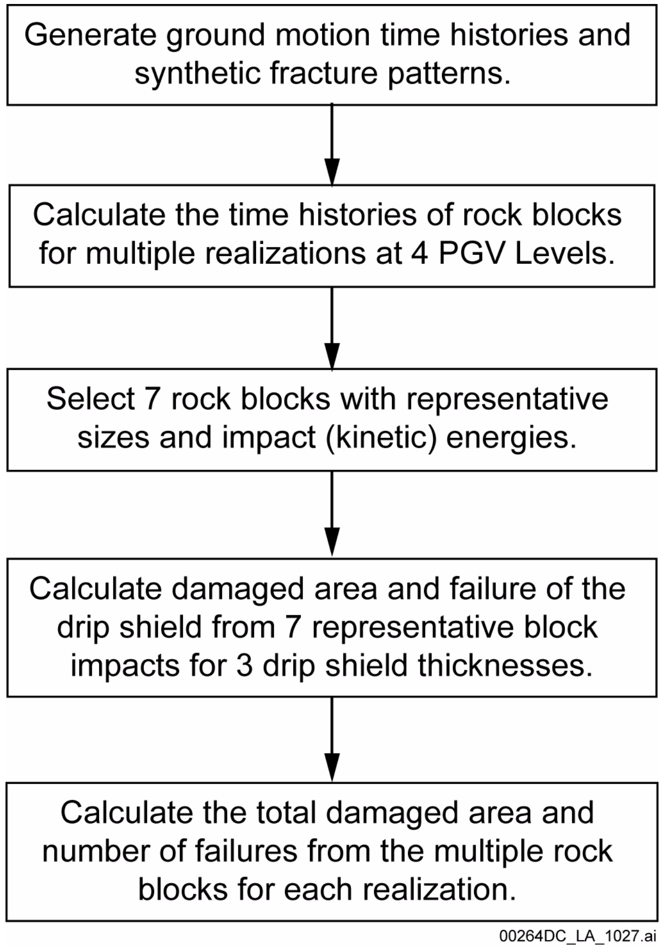


Figure 2.3.4-77. Methodology for Drip Shield Damage Abstraction from Rock Block Impacts

Source: SNL 2007c, Figure 6-98.

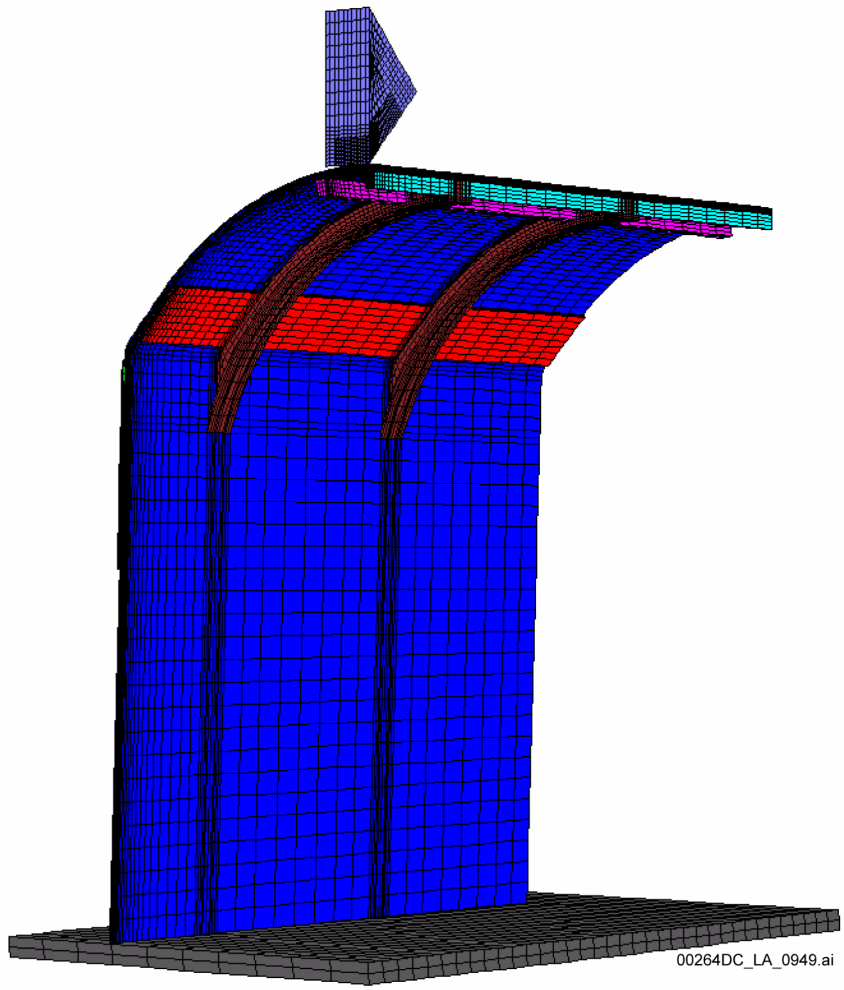


Figure 2.3.4-78. Impact Simulation of the 0.15 Metric Ton Block on the Drip Shield

NOTE: Block number 5, Table 2.3.4-34, represents the 70th percentile of impact energy at the 1.05 m/s PGV level ground motion level.

Source: SNL 2007b, Figure 6-73.

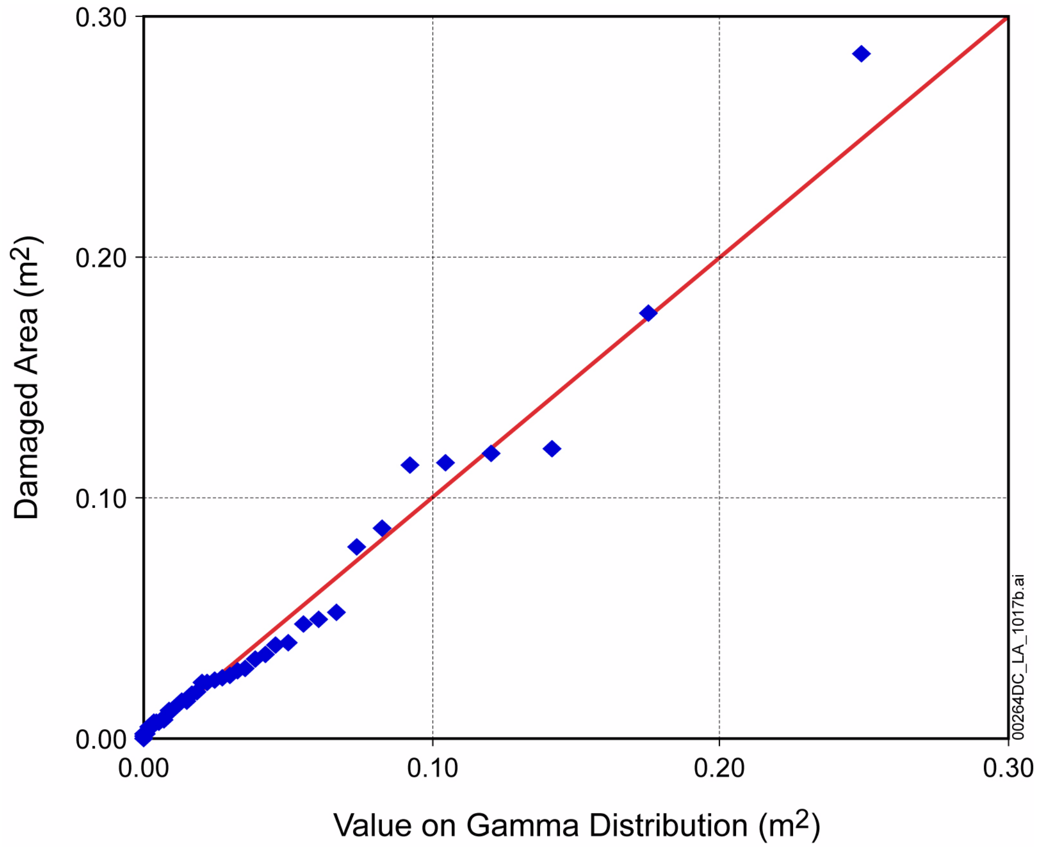


Figure 2.3.4-79. Q-Q Plot for Conditional Nonzero Damaged Area from Rock Block Impacts Versus a Gamma Distribution

NOTE: 2.44 m/s PGV level with 15-mm plate thickness. Damaged area is the conditional nonzero damaged area for each rockfall realization.

Source: SNL 2007c, Figure 6-99.

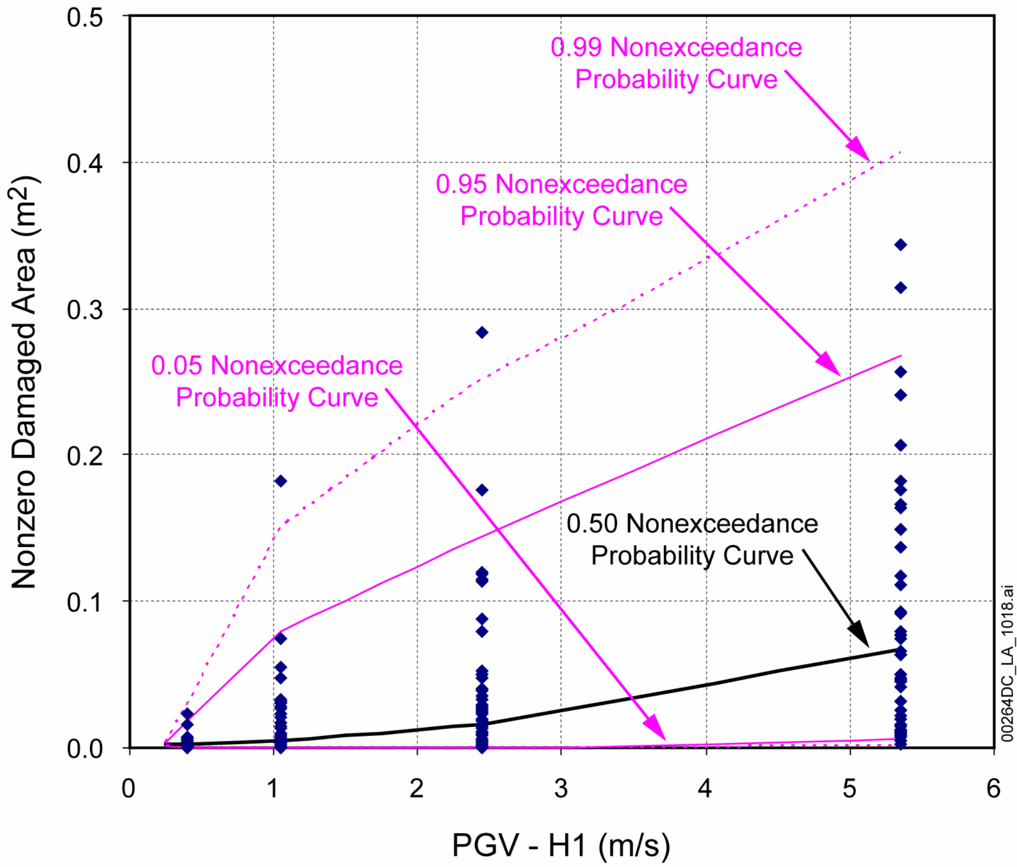


Figure 2.3.4-80. Comparison of Percentiles on the Gamma Distributions to Conditional Damaged Areas for the 15-mm-Thick Plates

NOTE: 15-mm plate thickness. The conditional nonzero damaged area is for each rockfall realization.

Source: SNL 2007c, Figure 6-102.

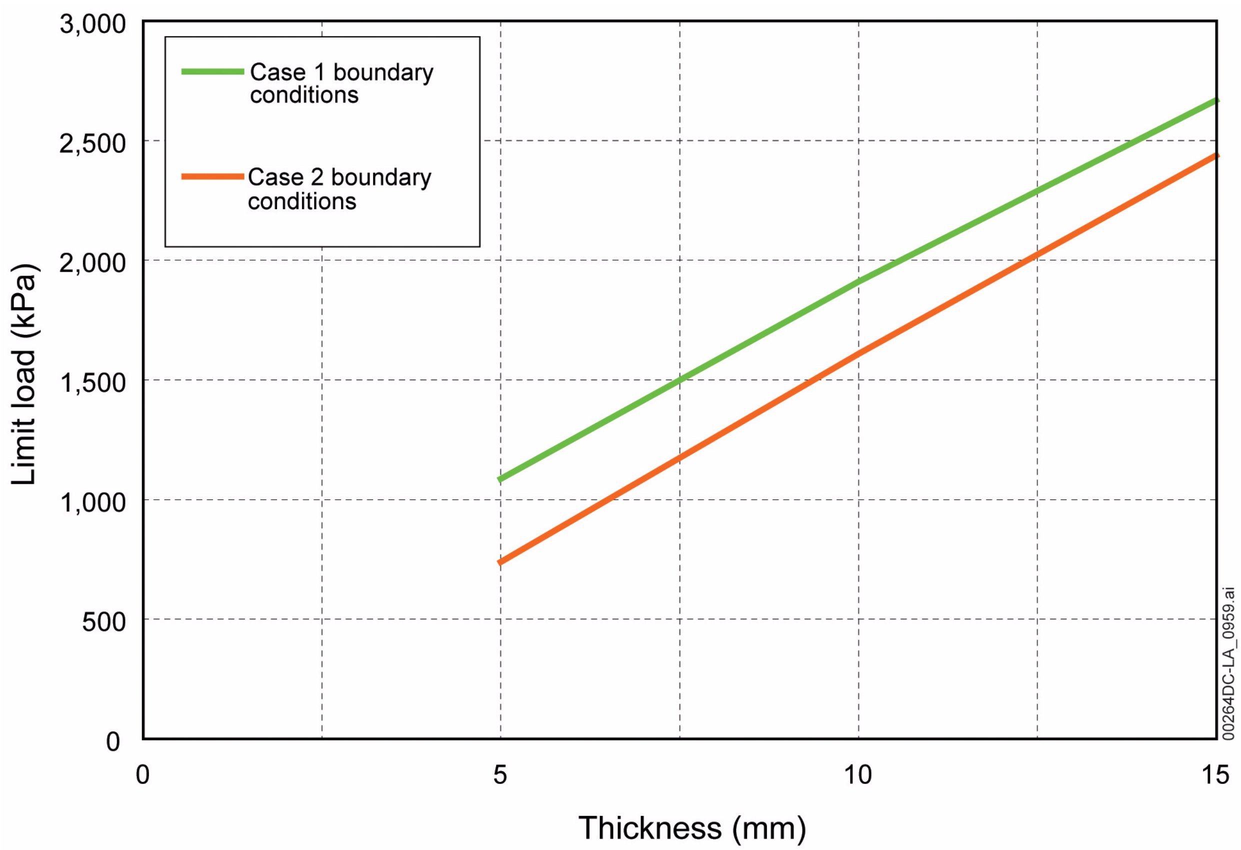


Figure 2.3.4-81. Fragility of the Drip Shield Plate as a Function of Plate Thickness and Boundary Conditions

Source: SNL 2007b, Figure 6-48.

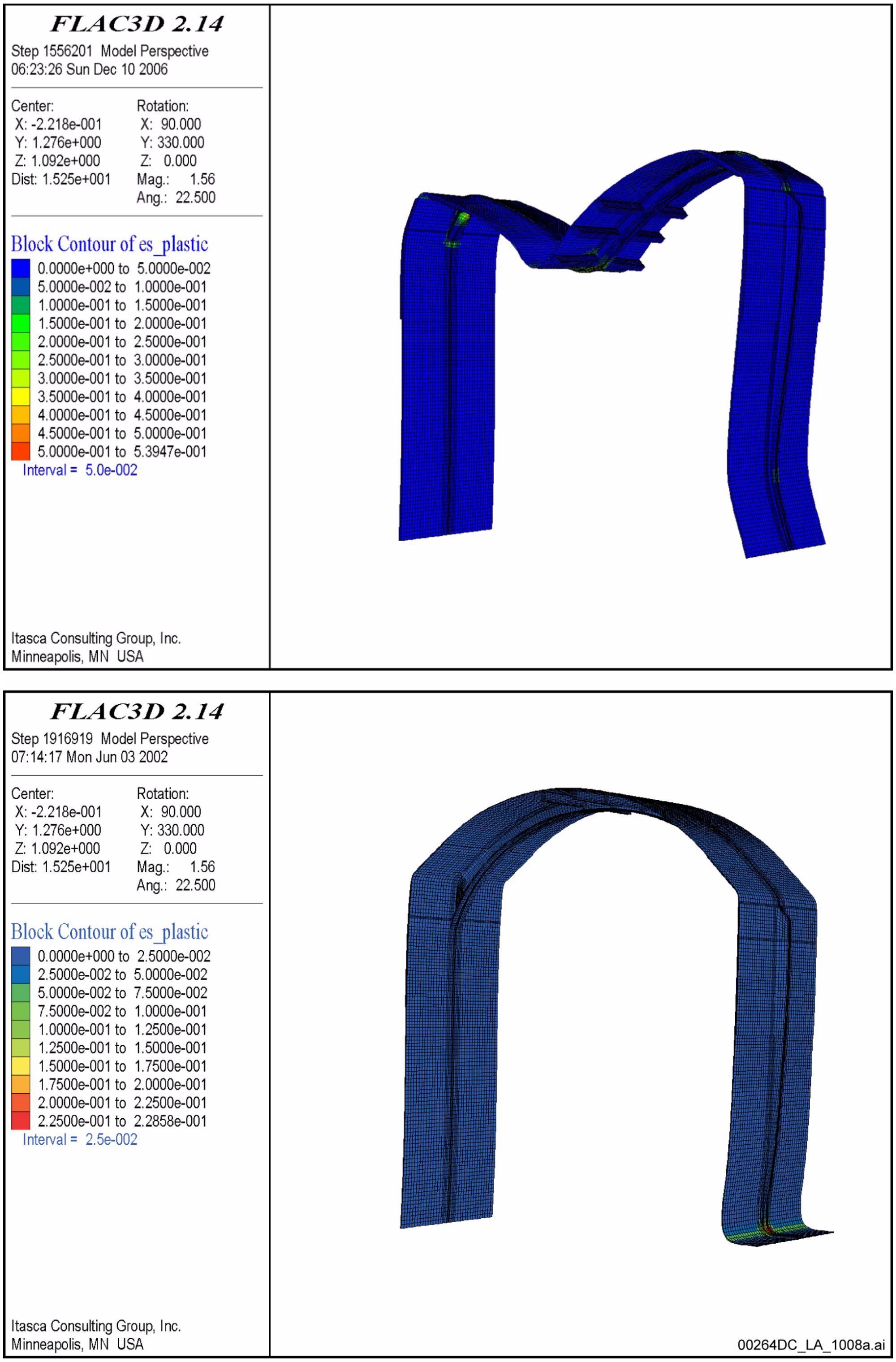


Figure 2.3.4-82. Deformed Shape and Contours of Plastic Shear Strain in the Failure State for the Drip Shield (top) Components Not Thinned, and, (bottom) Components Thinned 10 mm

NOTE: The applied rubble stress at drip shield failure for various framework thicknesses is given in Figure 2.3.4-83.

Source: SNL 2007b, Figures 6-54 and 6-56.

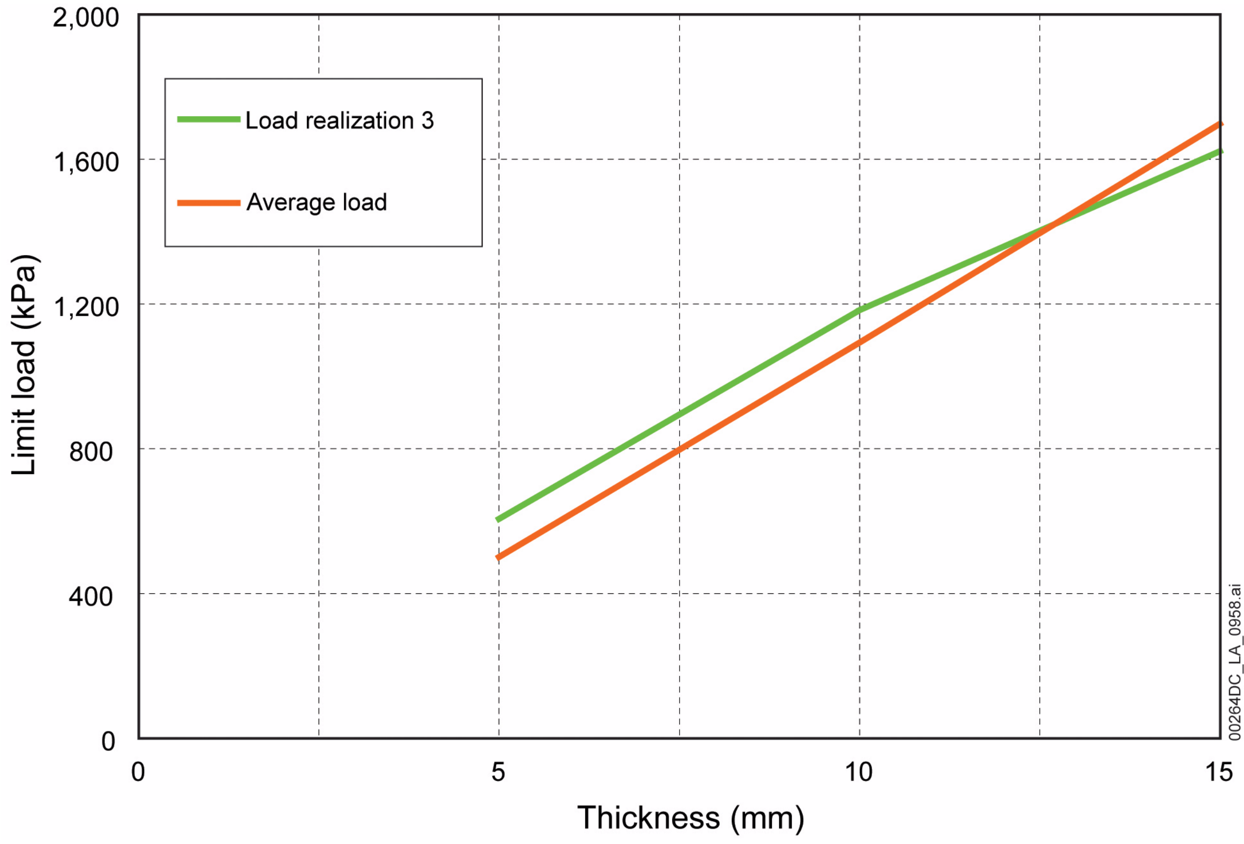


Figure 2.3.4-83. Limit Load of the Drip Shield Framework as a Function of Plate Thickness and Load Realization

NOTE: Thickness of all drip shield structural components reduced by the same amount as the thickness of the plates.

Source: SNL 2007b, Figure 6-57.

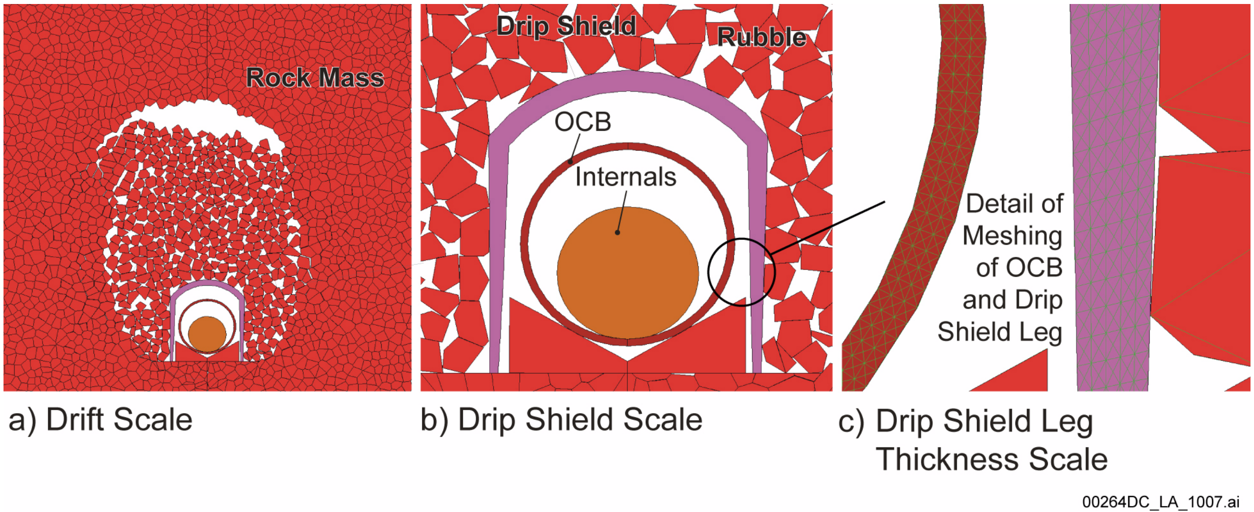


Figure 2.3.4-84. Geometrical Representation Used in the Analysis of the Mechanical Interaction Between the Drip Shield and the Rubble During Seismic Ground Motions

NOTE: The thickness of the structures in this diagram are not equivalent to actual design thicknesses of the actual structures. They have been adjusted so that the mechanical response of the 2D model approximates the 3D response (Section 2.3.4.5.3.3.3).

Source: SNL 2007b, Figure 6-58.

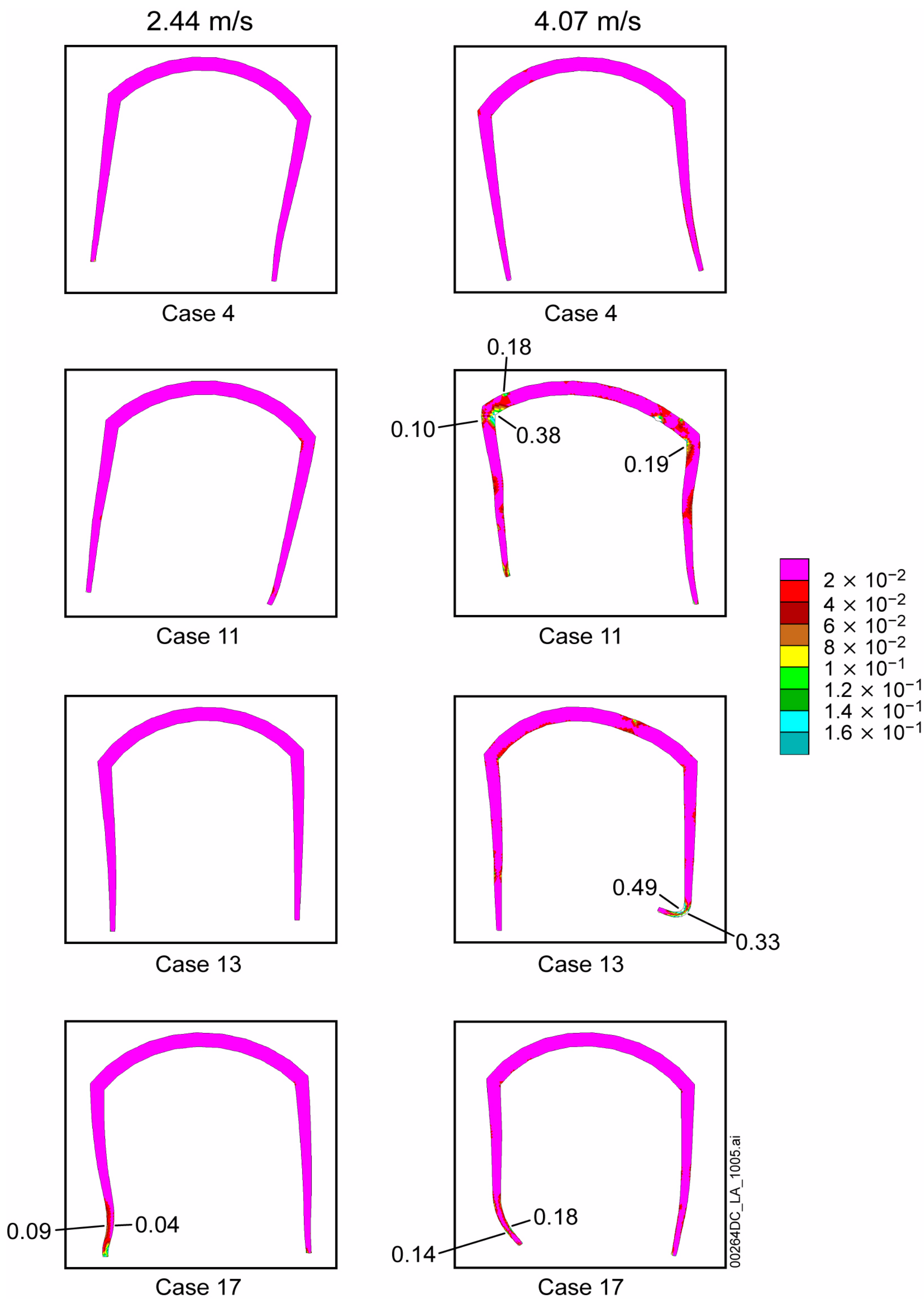


Figure 2.3.4-85. Example of the Deformed Drip Shield Geometries and Contours of Plastic Shear Strain for the Drip Shield Configuration When Components are Thinned 5 mm (Plate Thickness 10 mm)

NOTE: The maximum effective plastic strains (obtained by multiplying the plastic shear strain in the legend by $\sqrt{4/3}$ are shown numerically in the figures at locations of high distortion.)

Source: SNL 2007b, Figure 6-61.

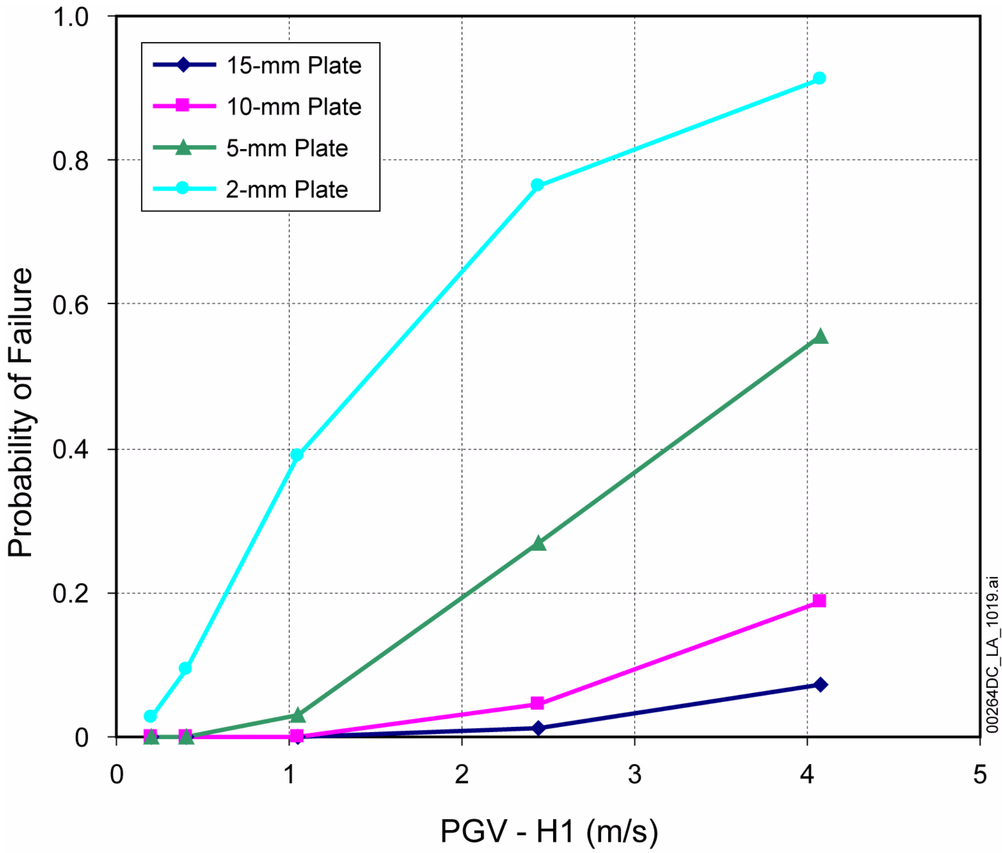


Figure 2.3.4-86. Probability of Failure of the Drip Shield Plates for Maximum Rockfall Load for Complete Drift Collapse

Source: SNL 2007c, Figure 6-71.

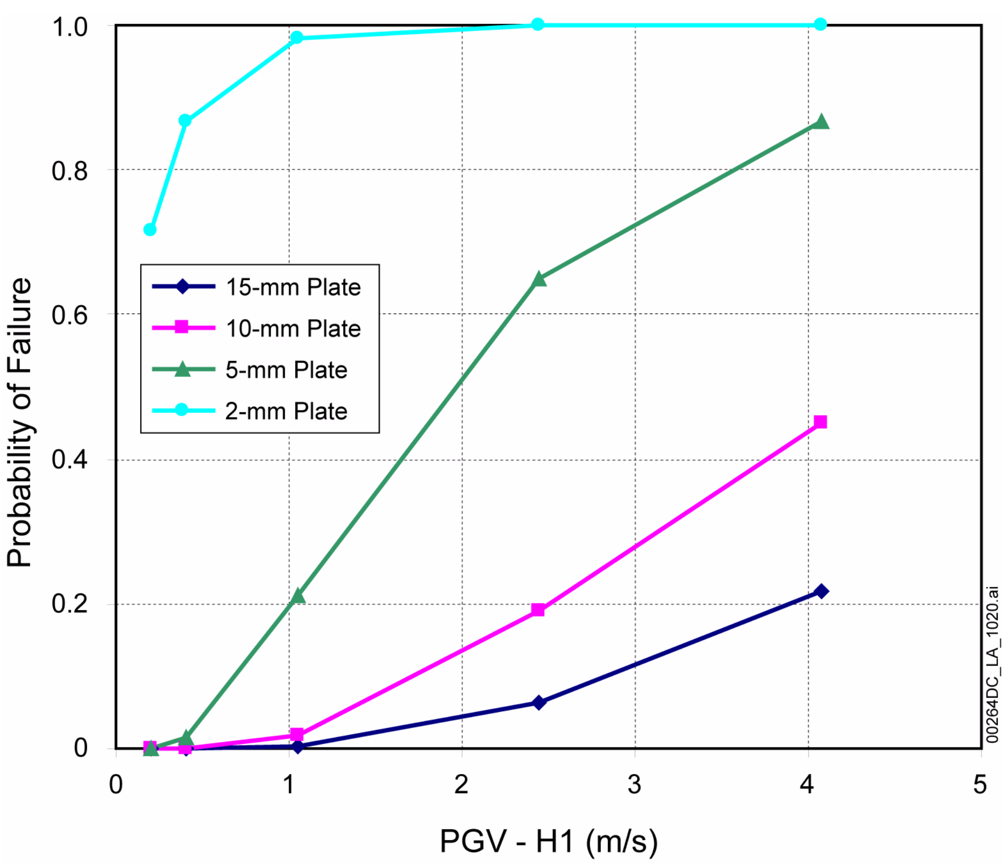


Figure 2.3.4-87. Probability of Collapse of the Drip Shield Framework for 100% Rockfall Load

Source: SNL 2007c, Figure 6-76.

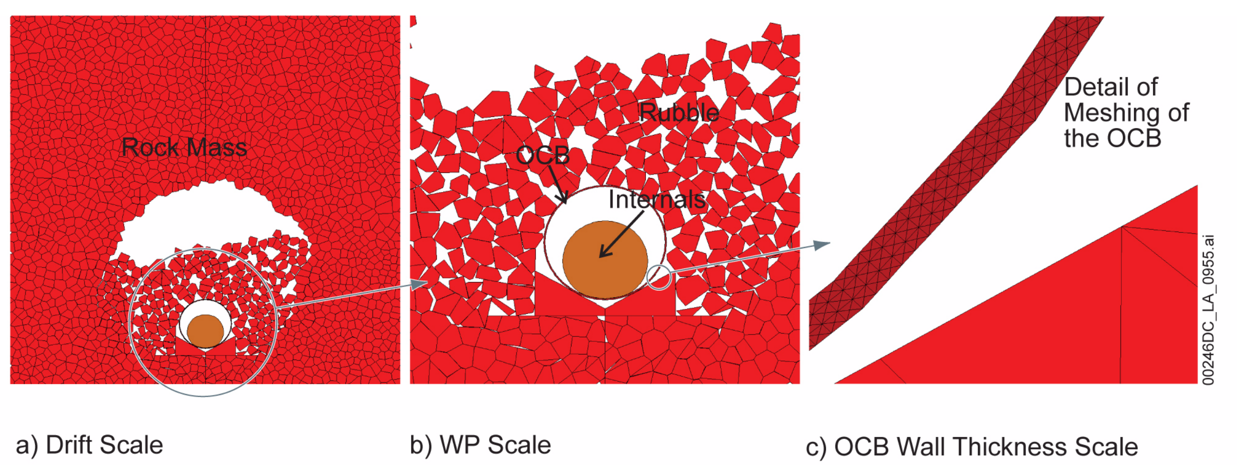


Figure 2.3.4-88. Geometrical Representation Used in the Analysis of the Mechanical Interaction Between the Waste Package and the Rubble During Seismic Ground Motions

Source: SNL 2007b, Figure 6-78.

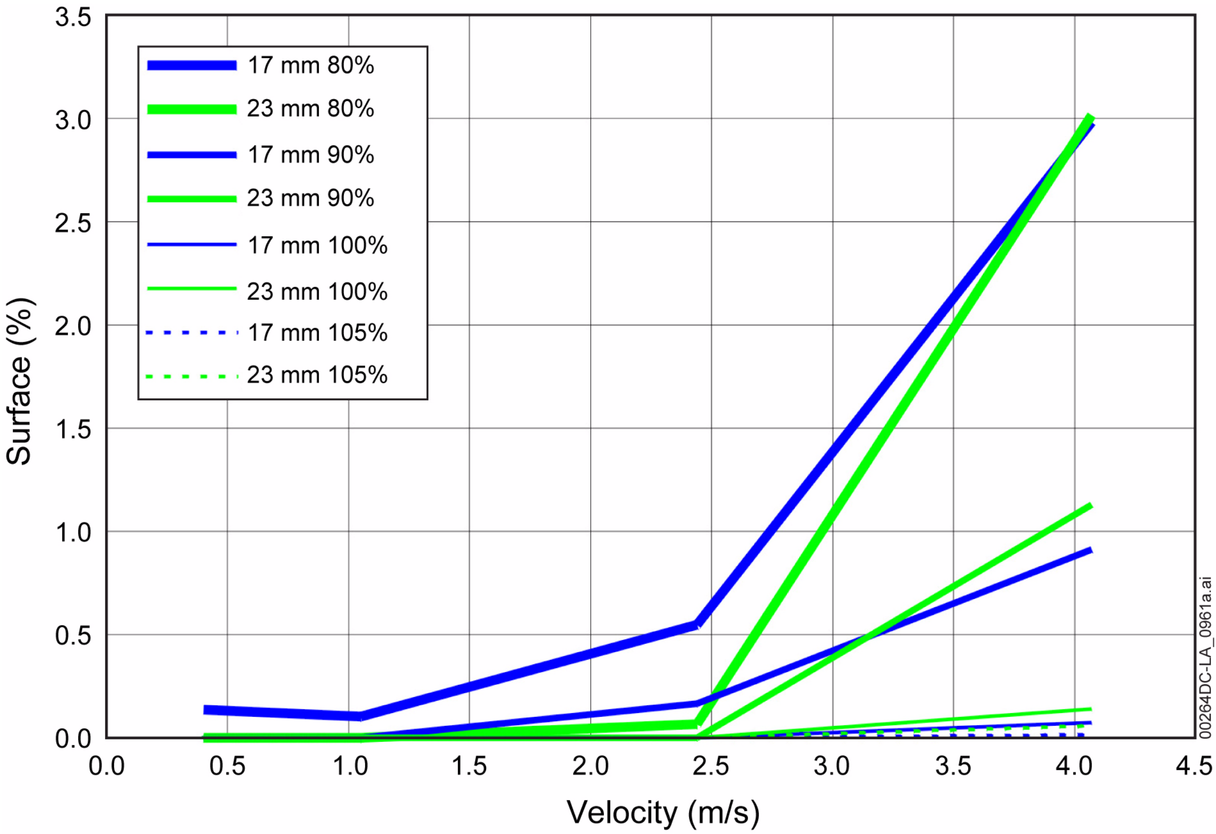


Figure 2.3.4-89. Average Damaged Surface Area for Two Outer Corrosion Barrier Thicknesses as a Function of PGV Level—Waste Package Surrounded by Rubble

NOTE: Values at 80% RST are not used in TSPA.

Source: SNL 2007b, Figure 6-88.

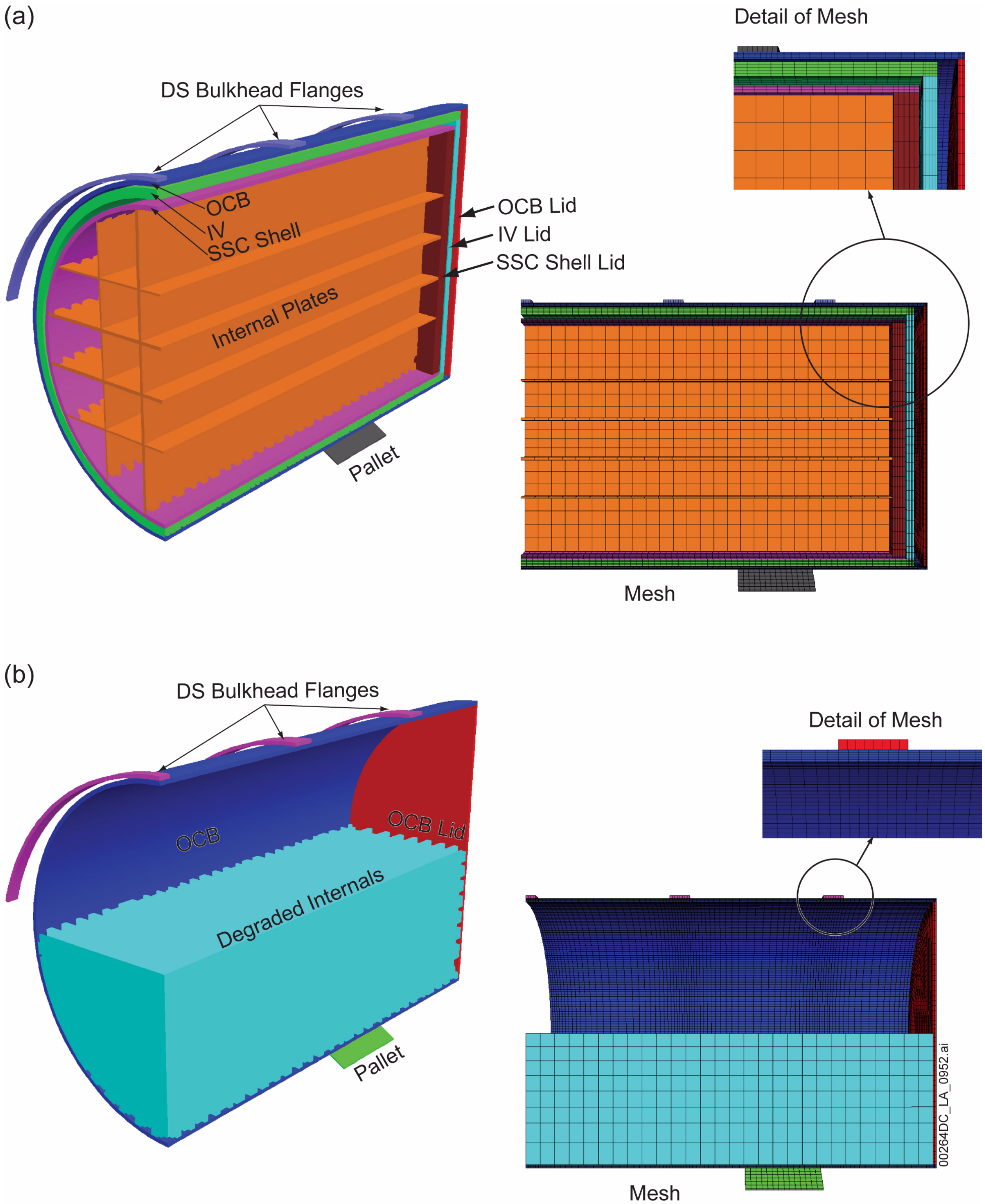


Figure 2.3.4-90. Geometrical Representation of the Waste Package Loaded by the Collapsed Drip Shield for the Case of Intact Internals (a) and Degraded Internals (b)

Source: SNL 2007b, Figures 6-89 and 6-90.

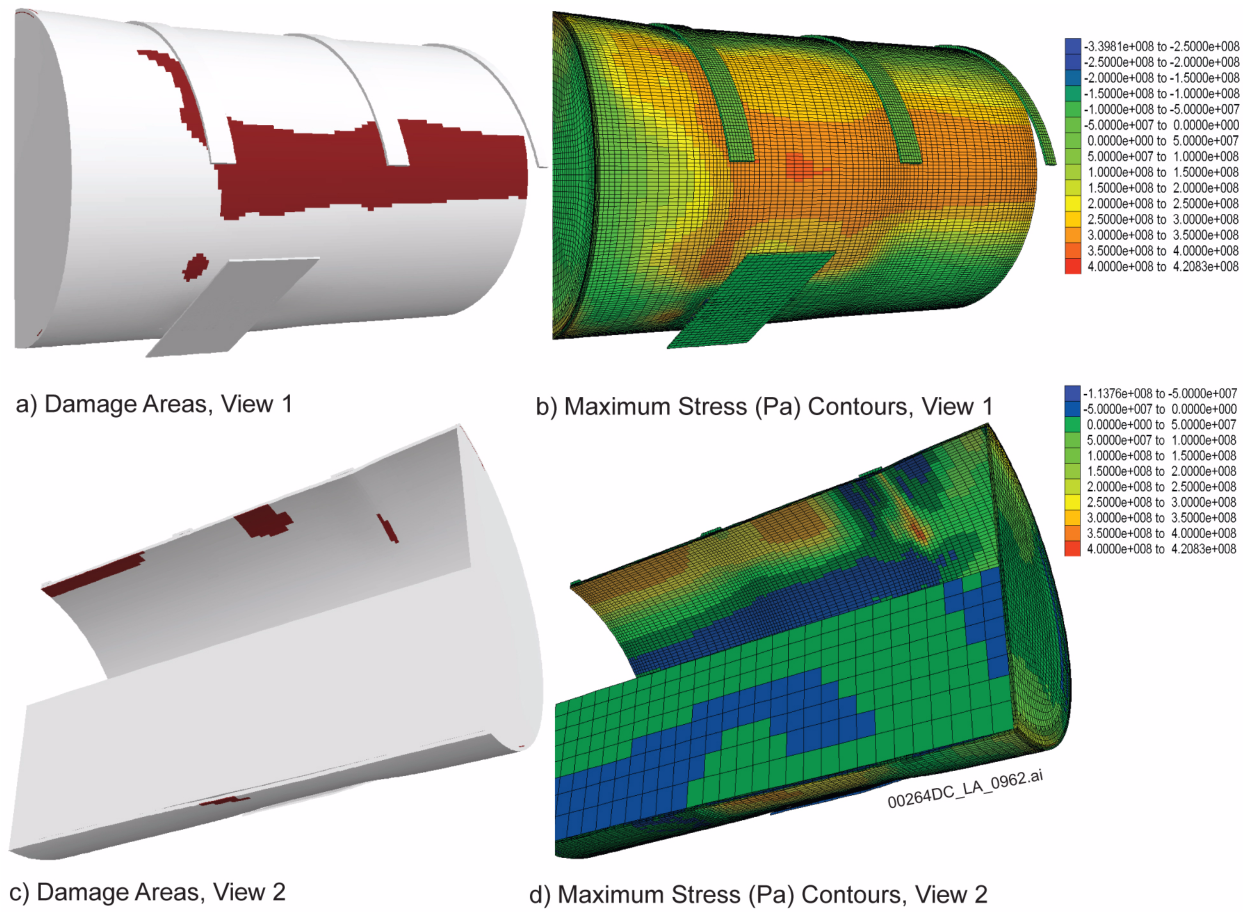


Figure 2.3.4-91. Damage Areas and Maximum Stress Contours Shown in Two Views for a 23-mm-Thick Outer Corrosion Barrier of the Waste Package with Degraded Internals Loaded by the Collapsed Drip Shield: 807 kPa Average Vertical Load

NOTE: The damage area is the inner or outer surface of the outer corrosion barrier with maximum stress greater than 90% of the yield strength of Alloy 22 (i.e., 316 MPa). The damage area is shown in brown.

Source: SNL 2007b, Figure 6-92.

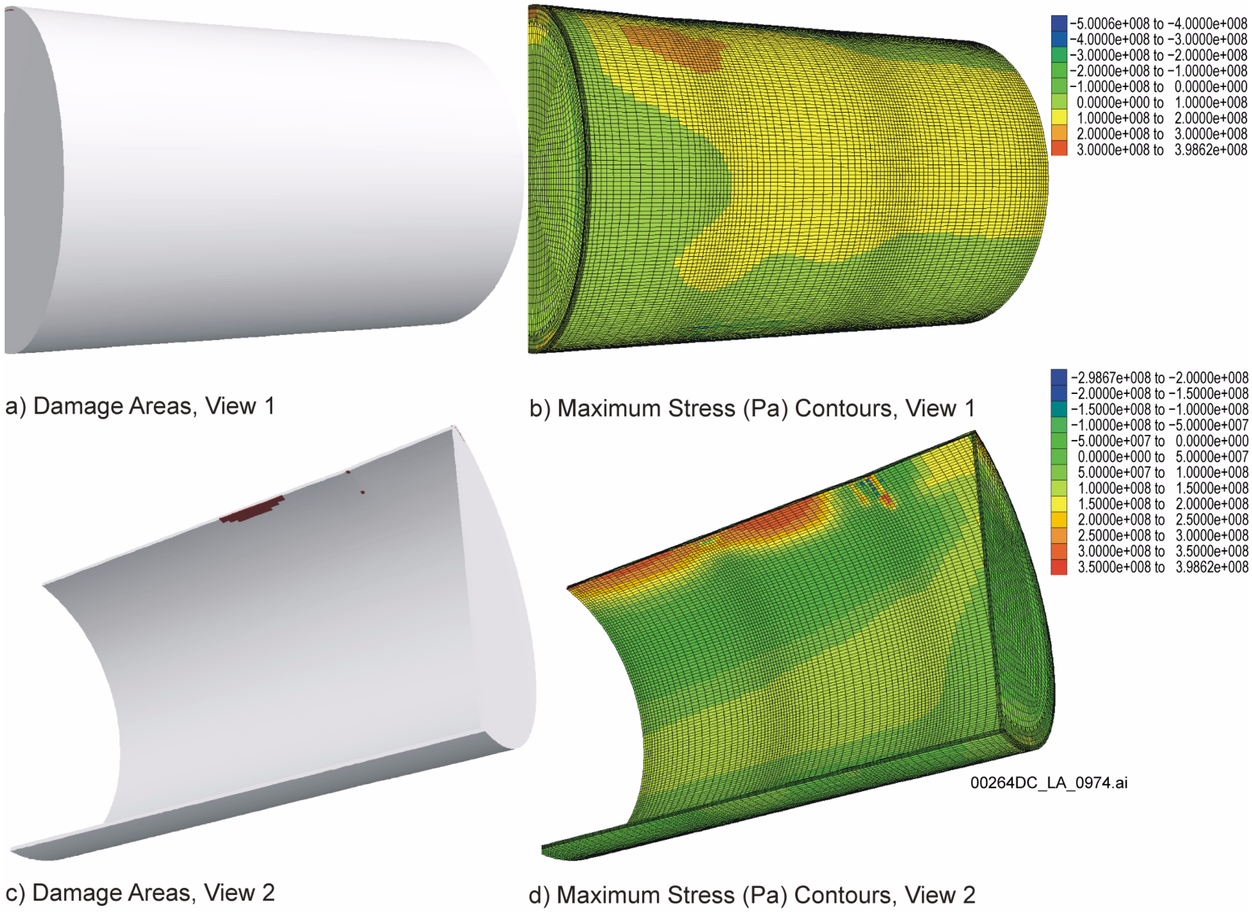


Figure 2.3.4-92. Damage Areas and Maximum Stress Contours Shown in Two Views for a 23-mm-Thick Outer Corrosion Barrier of the Waste Package with Intact Internals Loaded by the Collapsed Drip Shield: 1,483 kPa Average Vertical Load

NOTE: The damage area is the inner or outer surface of the outer corrosion barrier with maximum stress greater than 90% of the yield strength of Alloy 22 (i.e., 316 MPa). The damage area is shown in brown. The internals and pallet are not shown.

Source: SNL 2007b, Figure 6-93.

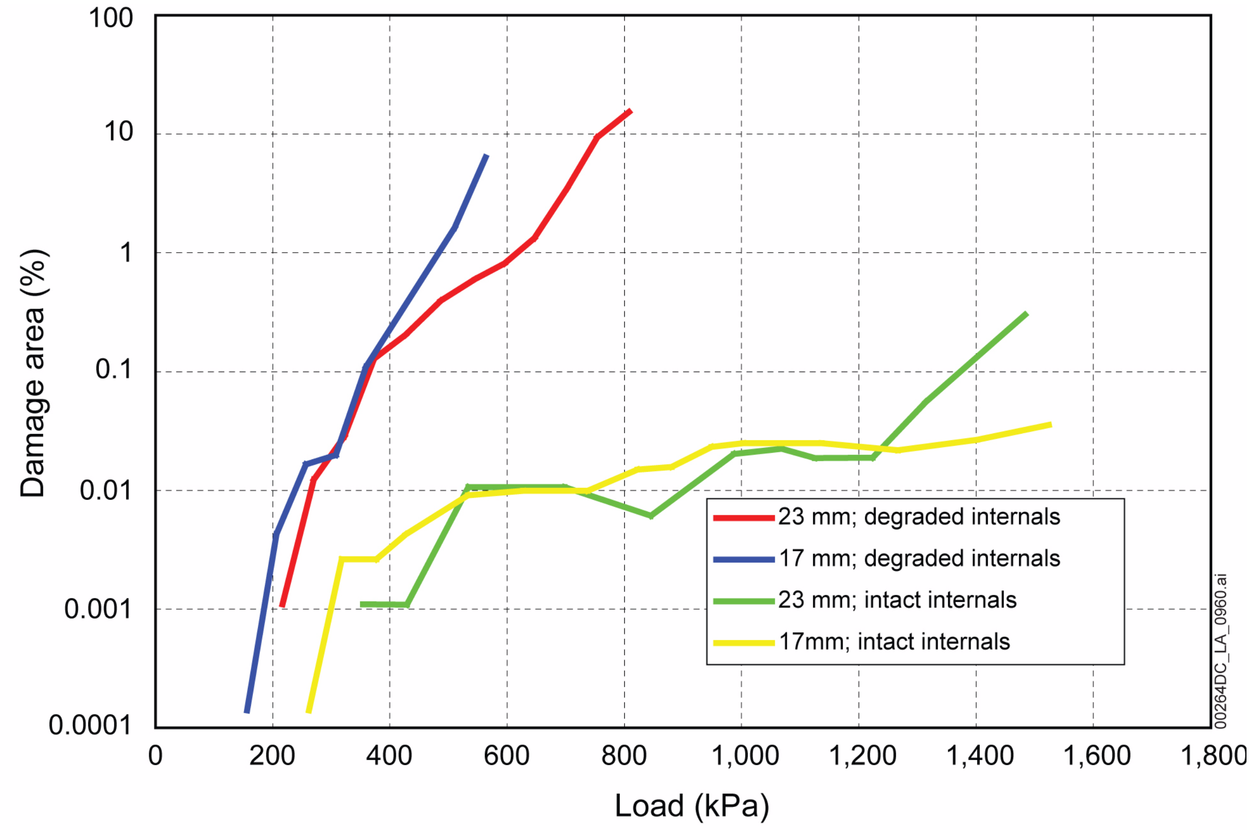


Figure 2.3.4-93. Surface Areas with Residual Stresses Greater than 90% of the Yield Strength of Alloy 22 ("Damage Area") as Function of Vertical Load for the Case of the Waste Package Loaded by the Collapsed Drip Shield for Two Outer Corrosion Barrier Thicknesses

Source: SNL 2007c, Figure 6-77.

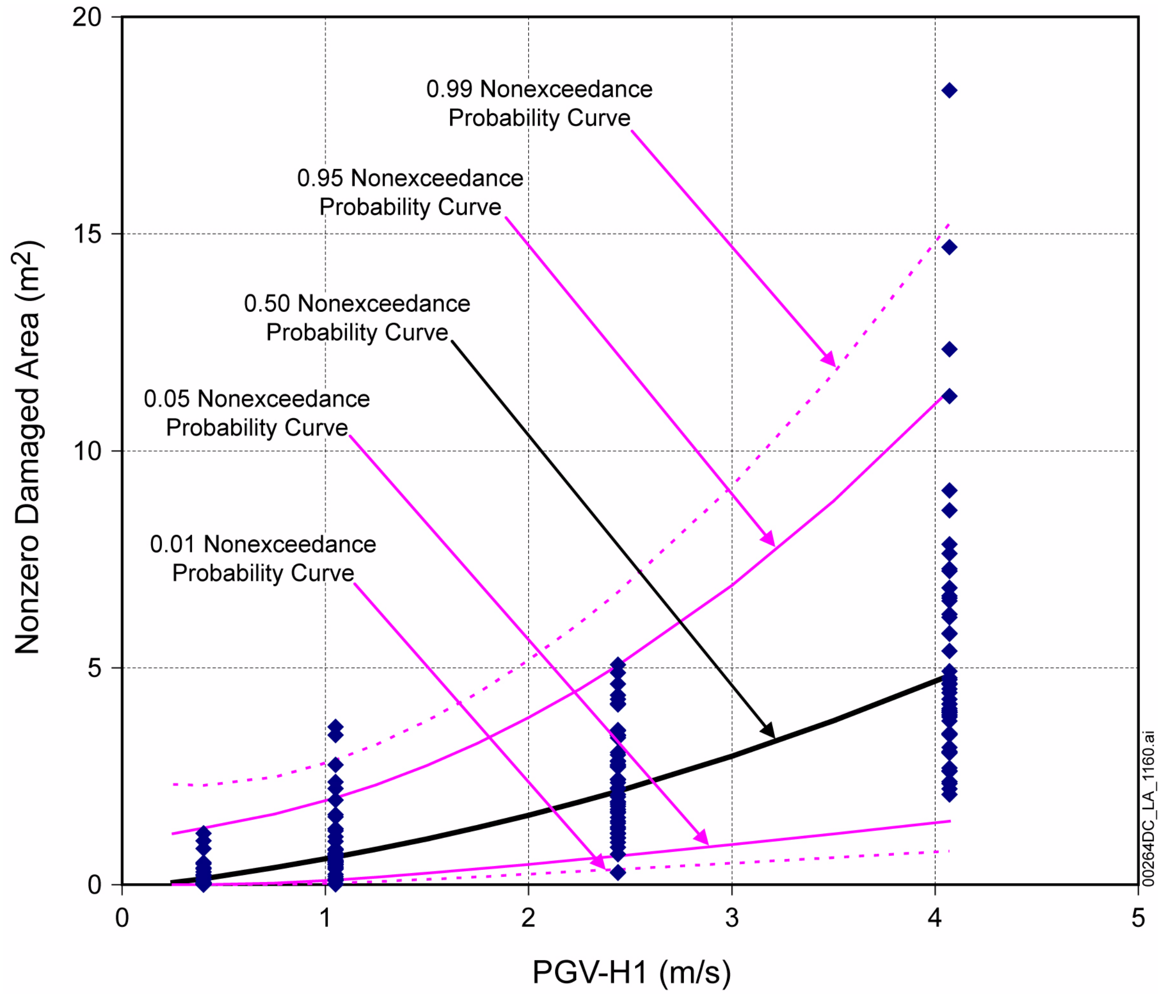


Figure 2.3.4-94. Comparison of Percentiles on the Gamma Distributions to Conditional Damaged Areas for the TAD-Bearing Waste Package with 17-mm-Thick Outer Corrosion Barrier and Degraded Internals

NOTE: 90% RST.

Source: SNL 2007c, Figure 6-20.

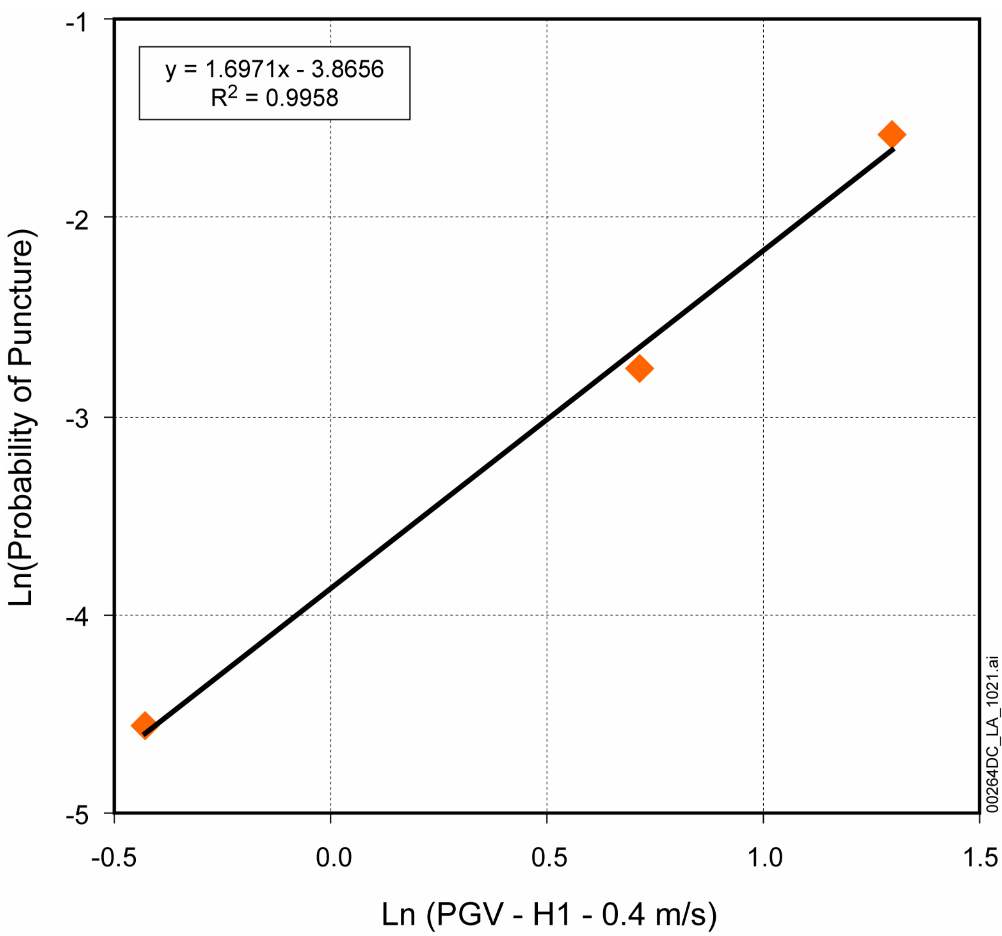


Figure 2.3.4-95. Least Squares Fit for Power Law Dependence for Probability of Puncture

NOTE: TAD-bearing waste package surrounded by rubble with 17-mm outer corrosion barrier and degraded internals.

Source: SNL 2007c, Figure 6-78.

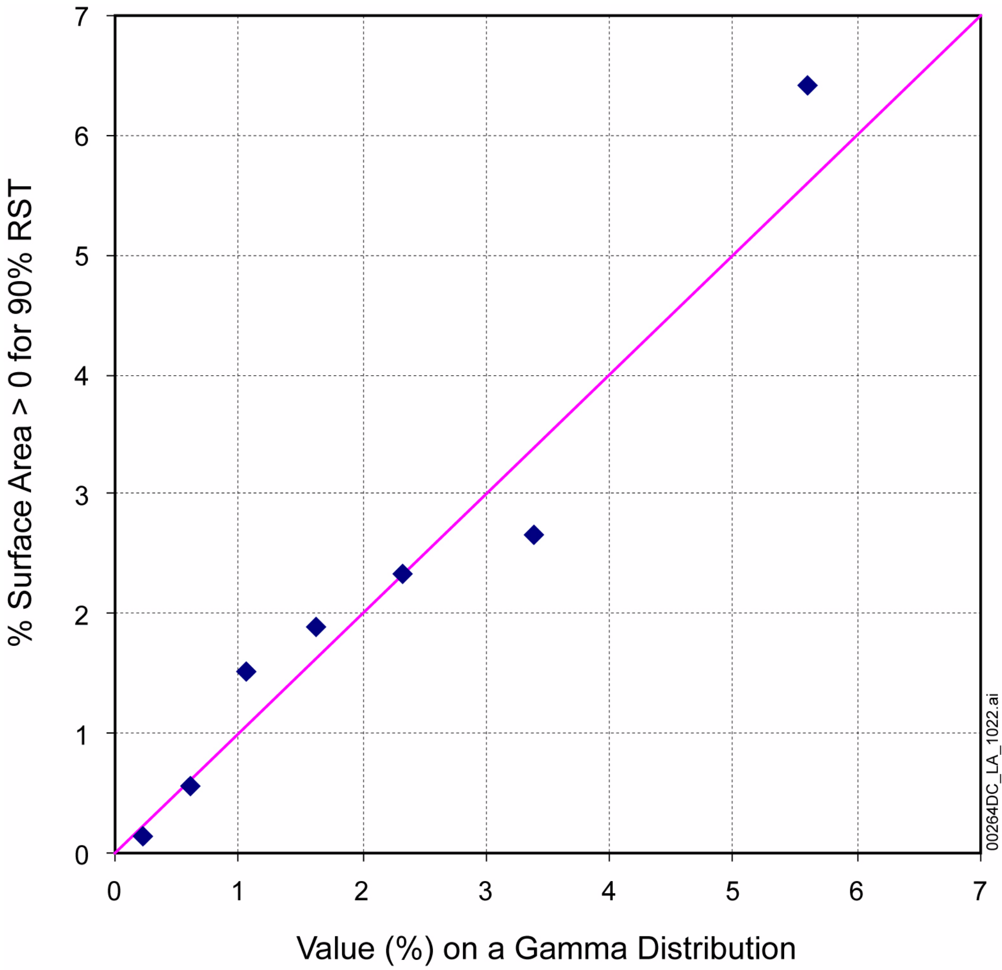


Figure 2.3.4-96. Q-Q Plot for Conditional Damaged Areas Versus a Gamma Distribution for the TAD-Bearing Waste Package Surrounded by Rubble

NOTE: 17-mm-thick outer corrosion barrier with degraded internals. 90% RST at the 4.07 m/s PGV level.

Source: SNL 2007c, Figure 6-82.

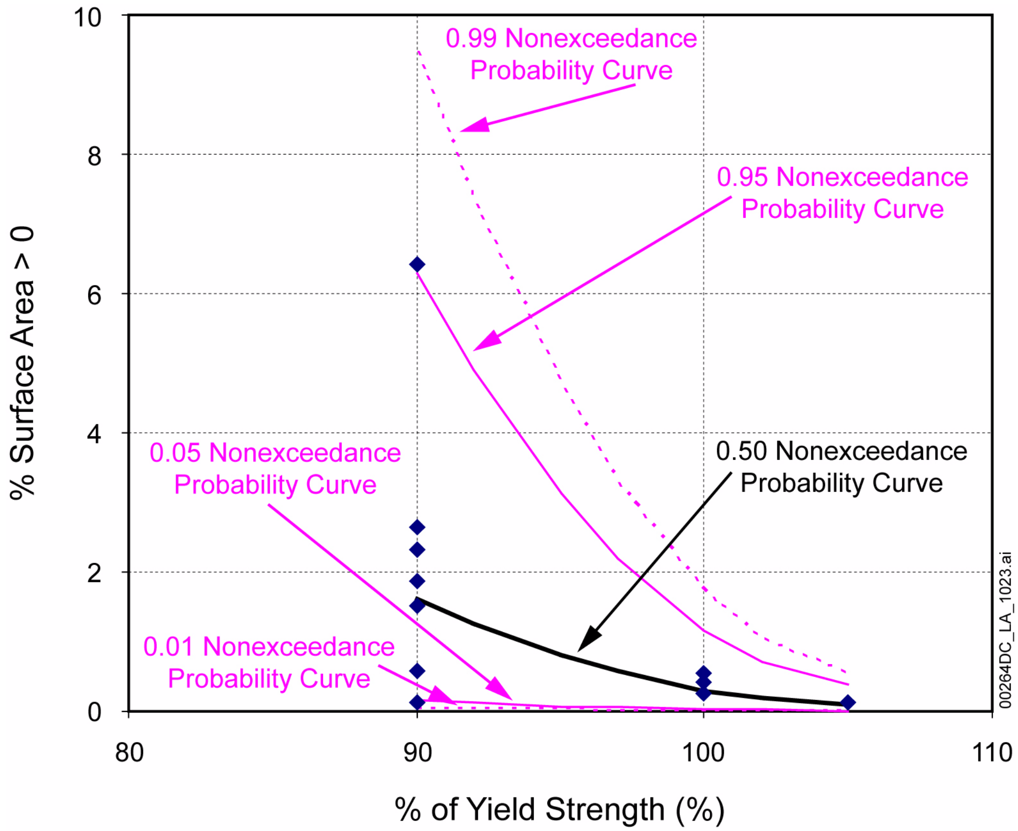


Figure 2.3.4-97. Comparison of Percentiles on the Gamma Distributions to Conditional Damaged Areas for the TAD-Bearing Waste Package Surrounded by Rubble

NOTE: 17-mm-thick outer corrosion barrier with degraded internals at the 4.07 m/s PGV level.

Source: SNL 2007c, Figure 6-85.

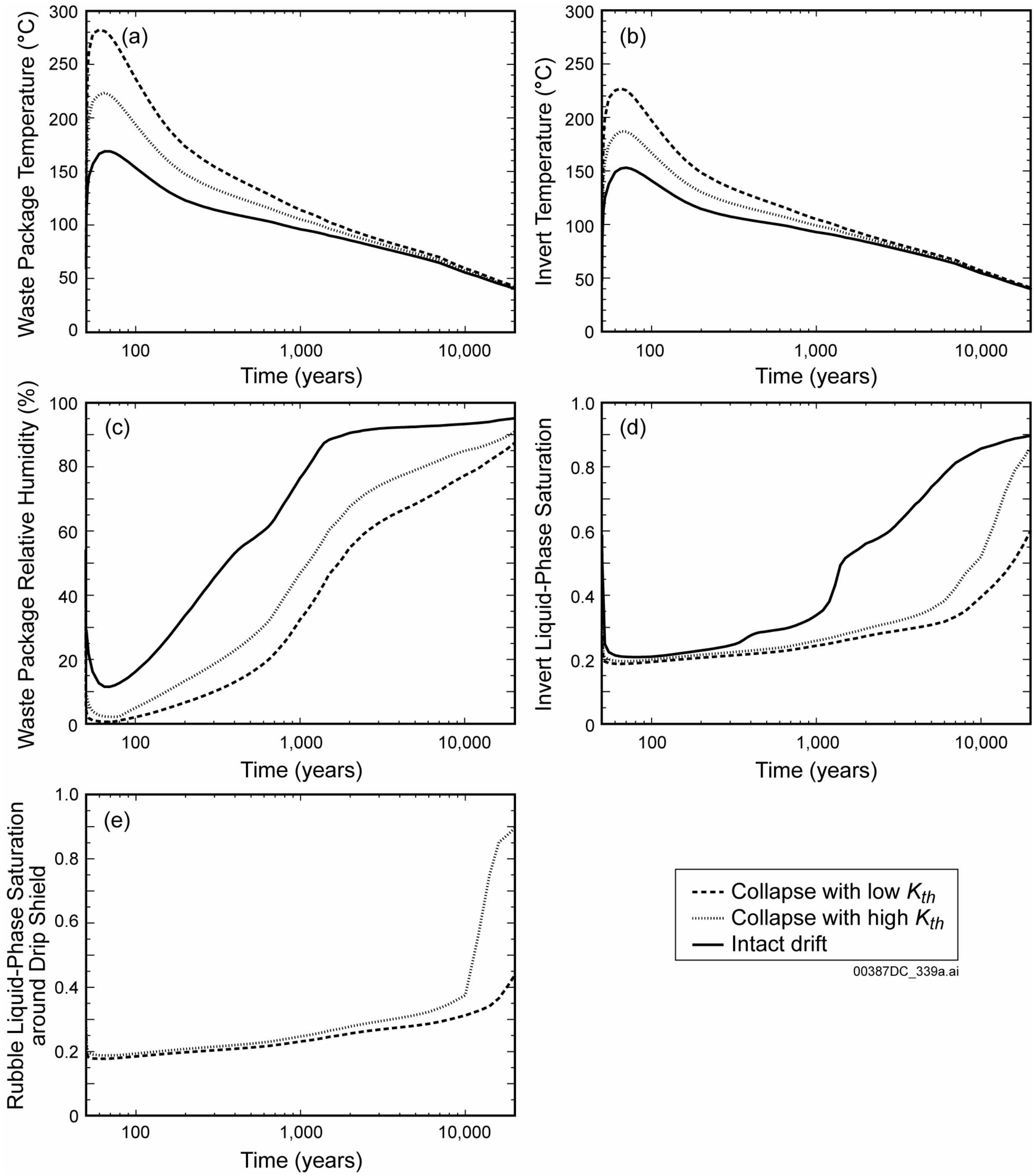


Figure 2.3.4-98. Thermal-Hydrologic Response for the 21-PWR Absorber Plate Waste Package

NOTE: Thermal-hydrologic response for the mean infiltration flux at the P2WR5C10 location, which is in the Tptpll (tsw35) unit (SNL 2008d, Figure 6.3-1 for location). The cases are: (1) intact-drift (nominal) case, (2) low-probability-seismic collapsed drift with high-Kth host-rock rubble, and (3) low-probability-seismic collapsed drift with low-Kth rubble. The plotted variables are (a) waste package temperature, (b) invert temperature, (c) waste package relative humidity, (d) invert liquid-phase saturation, and (e) matrix liquid-phase saturation of the rubble surrounding the drip shield.

Source: SNL 2008d, Figure 6.3-57.